Time-Periodic State Estimation with Event-Based Measurement Updates

Joris Sijs
TNO Technical Sciences
The Hague, Netherlands

Benjamin Noack
Karlsruhe Institute of Technology
Karlsruhe, Germany

Mircea Lazar
Eindhoven University of Technology
Eindhoven, Netherlands

Uwe D. Hanebeck
Karlsruhe Institute of Technology
Karlsruhe, Germany

CONTENTS

ABSTRACT To reduce the amount of data transfers in networked systems, measurements can be taken at an event on the sensor value rather than periodically in time. Yet, this could lead to a divergence of estimation results when only the received measurement values are exploited in a state estimation procedure. A solution to this issue has been found by developing estimators that perform a state update at both the event instants as well as periodically in time: when an event occurs the estimated state is updated using the measurement received, while at periodic instants the update is based on knowledge that the sensor value lies within a bounded subset of the measurement space. Several solutions for event-based state estimation will be presented in this chapter, either based on stochastic representations of random vectors, on deterministic representations of random vectors or on a mixture of the two. All solutions aim to limit the required computational resources

by deriving explicit solutions for computing estimation results. Yet, the main achievement for each estimation solution is that stability of the estimation results are (not directly) dependent on the employed event sampling strategy. As such, changing the event sampling strategy does not imply to change the event-based estimator as well. This aspect is also illustrated in a case study of tracking the distribution of a chemical compound effected by wind via a wireless sensor network.

13.1 Introduction

Many people in our society manage their daily activities based on knowledge and information about weather conditions, traffic jams, pollution levels, energy consumptions, stock exchange, and so on. Sensor measurements are the main source of information when monitoring these surrounding processes, and a trend is to increase their amount, as they have become smaller, cheaper, and easier to use. See, for example, detailed explanations on the design of "wireless sensor networks" and its applications in [7]. As many more sensor measurements are becoming available, resource limitations of the overall system are gradually becoming the bottleneck for processing measurements automatically. The main reason for this issue is that classical signal processing solutions have been developed in a time where sensor measurements were scarce and where systems were deployed with sufficient resources for running sophisticated algorithms developed. Nowadays, these aspects are shifted, that is, there are far too many sensor measurements available for the limited resources deployed in the overall system and, moreover, it is typically not even necessary to process all sensor information available to achieve a desired performance. An example of resource-aware signal processing is presented in this chapter, where several solutions for state estimation will be presented that all aim to reduce the amount of measurement samples.

More precisely, this chapter presents a recent overview and outlook on state estimation approaches that do not require periodic measurement samples but instead were designed for exploiting a-periodic measurement samples. Some well-known a-periodic sampling strategies, known as *event-based sampling* or *event triggered sampling*, are "send-on-delta" (or Lebesgue sampling) and "integral sampling" proposed in [3,10,22,23]. When such strategies are used in estimation (and control), as will be the case in this chapter, one typically starts with the setup depicted in Figure 13.1. Note that the sensor may require access to estimation results of the estimator, for example, in case the event sampling strategy "matched sampling" of [20] is employed.

Typically, the estimator is part of a larger networked system where the output of the estimator is used by a control algorithm for computing stabilizing control actions. Advances in control theory provided several solutions for coping with the event sampled measurements directly by the controller. See, for example, the solutions on event-based control proposed in [5,8–10,12,14,16,33,37]. Yet, most of the deployed controllers used in current practices run periodically in time. Revisiting those periodic controller into an event-based one is not favorable. Mainly because the infrastructure of the control system is inflexible or because of fear for any down-time of the production facility when new controllers are tested.

The event-based estimators addressed in this chapter can serve as a solution to this problem:

- Event-based sensor measurements are sent to the estimator.
- Estimation results are computed at events *and* periodically in time.
- The time-periodic estimation results are sent to the controller.
- Stabilizing control actions are computed periodically in time.

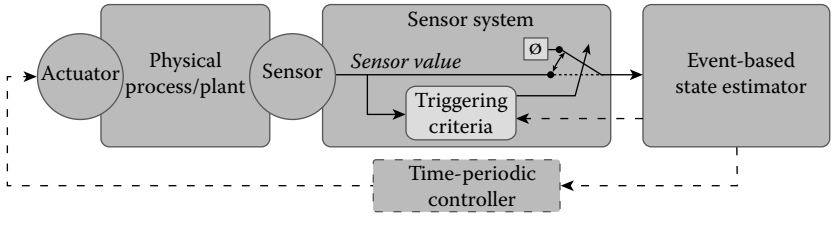

FIGURE 13.1

Schematic setup of event-based state estimation (and control). Therein, a sensor system studies the sensor signal on events in line with a predefined "event triggering criteria." In case of the event, the sensor signal is sampled and the corresponding measurement is sent to the estimator. In case of no event, no measurement is sent (represented by an empty set $\emptyset$ at the input of the estimator). The estimator exploits the event-triggered sensor measurements to compute time-periodic estimation results, which are possibly used by a time-periodic controller for computing stabilizing control actions.

The advantage of such an approach is twofold. First, the design of a (practical) stabilizing controller becomes independent from the employed event sampling strategy and existing control implementations might even be kept in the loop when changing from time-periodic to event-based measurements. Secondly, one can select a suitable control approach from the extensive set of time-periodic control algorithms. The purpose of this article is to assess existing event-based state estimators for time-periodic observations and apply them in an environmental monitoring application.

13.2 Preliminaries

$\mathbb{R}$, $\mathbb{R}_+$, $\mathbb{Z}$, and $\mathbb{Z}_+$ define the sets of real numbers, nonnegative real numbers, integer number, and nonnegative integer numbers, respectively, while, $\mathbb{Z}_{\mathbb{C}} := \mathbb{Z} \cap \mathbb{C}$, for some $\mathbb{C} \subset \mathbb{R}$. An ellipsoidal set $\mathbb{L}_{(\mu,\Sigma)} \subset \mathbb{R}^n$ centered at $\mu \in \mathbb{R}^n$ is characterized as $\mathbb{L}_{\mu,\Sigma} := \{x \in \mathbb{R}^l | (x-\mu)^\top \Sigma^{-1}(x-\mu) \leq 1\}$, for some positive definite $\Sigma \in \mathbb{R}^{n\times n}$. The Minkowski sum of two sets $\mathbb{C}_1, \mathbb{C}_2 \in \mathbb{R}^n$ is denoted as $\mathbb{C}_1 \oplus \mathbb{C}_2 := \{x + y | x \in \mathbb{C}_1, y \in \mathbb{C}_2\}$. The null-matrix and identity-matrix of suitable dimensions (clear from the context) are denoted as 0 and I, respectively. For a continuous-time signal $x(t)$, where $t_{\mathsf{k}} \in \mathbb{R}_+$ denotes the time of the k-th sample, let us define $x[\mathsf{k}] := x(t_{\mathsf{k}})$ and $x(t_{0:\mathsf{k}}) := (x(t_0), x(t_1), \cdots, x(t_{\mathsf{k}}))$. The q-th element of a vector $x \in \mathbb{R}^n$ is denoted as $\{x\}_q$, while $\{A\}_{qr}$ denotes the element of a matrix $A \in \mathbb{R}^{m\times n}$ in the q-th row and r-th column. The transpose, determinant, inverse, and trace of a matrix $A \in \mathbb{R}^{n\times n}$ are denoted as $A^\top$, $|A|$, A^{-1}, and $\mathrm{tr}(A)$, respectively. The minimum and maximum eigenvalue of a square matrix A are denoted as $\lambda_{\min}(A)$ and $\lambda_{\max}(A)$, respectively. The p-norm of a vector $x \in \mathbb{R}^n$ is denoted as $\|x\|_p$.

The Delta-function $\delta : \mathbb{R}^n \to \mathbb{R}_+$ of a vector $x \in \mathbb{R}^n$ vanishes at all values of $x \neq 0$, while it is infinity when $x = 0$ and, moreover, $\int_{-\infty}^{\infty} \delta(x)\mathrm{d}x = 1$.

The probability density function (PDF) of a random vector $x \in \mathbb{R}^n$ is denoted as $p(x)$, while $x \sim \mathcal{G}(\mu, \Sigma)$ is a short notation for stating that the PDF of x is a Gaussian function with mean $\mu \in \mathbb{R}^n$ and covariance $\Sigma \in \mathbb{R}^{n\times n}$, that is, $p(x) = \mathcal{G}(x, \mu, \Sigma)$ and $\mathcal{G}(x, \mu, \Sigma) := \frac{1}{\sqrt{(2\pi)^n|\Sigma|}} e^{-0.5(x-\mu)^\top \Sigma^{-1}(x-\mu)}$. Further, for a bounded Borel set $\mathbb{C} \subset \mathbb{R}^n$ [1], the corresponding uniform PDF $\Pi_{\mathbb{C}}(x) : \mathbb{R}^n \to \mathbb{R}_+$ is characterized by $\Pi_{\mathbb{C}}(x) = 0$ if $x \notin \mathbb{C}$ and $\Pi_{\mathbb{C}}(x) = \nu^{-1}$ if $x \in \mathbb{C}$, with $\nu \in \mathbb{R}$ defined as the Lebesgue measure of $\mathbb{C}$ [15].

13.3 A Hybrid System Description: Event Measurements into Time-Periodic Estimates

Event-based state estimation with time-periodic estimation results deals with the setup depicted in Figure 13.1, that is, a sensor system forwarding sampled measurements to a state estimator that is possibly connected to a control implementation. Important prerequisites for the event-based state estimator in the schematic set-up of Figure 13.1 are the sampling strategies employed and the physical process considered.

Event triggered sampling The sensor system employs an event triggering criteria to generate a next measurement $y \in \mathbb{R}^m$ at the event instants $t_{\mathsf{e}} \in \mathbb{R}_+$, where $\mathsf{e} \in \mathbb{Z}_+$ denotes the e-th event sample. To that extent, let $\mathbb{T}_e \subset \mathbb{R}_+$ be the collection of time instants at all events, that is ,

$$\mathbb{T}_e := \{t_{\mathsf{e}} \in \mathbb{R}^n \mid \mathsf{e} \in \mathbb{Z}_+\}.$$

Further, let us introduce $\tau_{\mathsf{e}} := t_{\mathsf{e}} - t_{\mathsf{e}-1}$ as the sampling interval between two consecutive events e and $\mathsf{e}-1$. A definition of the event instants t_{e} is given in the next section.

Time-periodic sampling The control implementation employs a time-periodic sampling strategy characterized by a constant sampling interval $\tau_s \in \mathbb{R}_{>0}$. To that extent, let $\mathbb{T}_p \subset \mathbb{R}_+$ be the collection of periodic time instants, that is,

$$\mathbb{T}_p := \{\mathsf{n}\tau_s \mid \mathsf{n} \in \mathbb{Z}_+\}.$$

Notice that event instants could coincide with time-periodic instants, that is, $\mathbb{T}_e \cap \mathbb{T}_s$ might be non-empty.

Physical process Let us consider an autonomous, linear process discretized in time for various sampling intervals $\tau \in \mathbb{R}_{>0}$:

$$x(t) = A_\tau x(t-\tau) + B_\tau w(t), \tag{13.1}$$
$$y(t) = Cx(t) + v(t). \tag{13.2}$$

Basically, the above description could be perceived as a discretized version of a continuous time state-space model $\dot{x}(t) = Fx(t) + Ew(t)$, where $A_\tau := e^{F\tau}$ and $B_\tau := \int_0^\tau e^{F\eta} d\eta E$. The state vector is denoted as $x \in \mathbb{R}^n$ and both the process noise $w \in \mathbb{R}^l$ and measurement noise $v \in \mathbb{R}^m$ are characterized with a deterministic part and a stochastic part, that is,

$$w(t) := w_d(t) + w_s(t) \quad \text{and} \quad v(t) := v_d(t) + v_s(t).$$

Herein, $w_d(t) \in \mathbb{W}$ and $v_d(t) \in \mathbb{V}$ denote "deterministic," yet unknown, vectors taking values in the

sets $\mathbb{W} \in \mathbb{R}^l$ and $\mathbb{V} \in \mathbb{R}^m$. Further, $w_s(t) \in \mathbb{R}^l$ and $v_s(t) \in \mathbb{R}^m$ denote "stochastic" random vectors taking values according to the PDFs $p(w_s(t))$ and $p(v_s(t))$. Exact characterizations of $\mathbb{W}$, $\mathbb{V}$, $p(w_s)$, and $p(v_s)$ vary per estimation approach and will be discussed in the preceding sections. Still, it is important to note that an *unbiased* noise $w(t)$ and $v(t)$ implies that both $\mathbb{W}$ and $\mathbb{V}$ have their center-of-mass collocated with the origin and that both $w_s(t)$ and $v_s(t)$ have an expected value of zero.

The purpose of the state estimator is to exploit the event measurements y to compute an estimate of the state x. In line with the above noise characterizations, estimation results of the event-based state estimator are also represented with a deterministic and a stochastic part, that is,

$$x(t) := \hat{x}(t) + \tilde{x}_d(t) + \tilde{x}_s(t).$$

Herein, $\hat{x} \in \mathbb{R}$ is the estimated mean of x and both $\tilde{x}_d, \tilde{x}_s \in \mathbb{R}^n$ are estimation errors, that is, $\tilde{x}_d + \tilde{x}_s = x - \hat{x}$. More precisely, $\tilde{x}_d(t) \in \mathbb{X}$ is a deterministic, yet unknown, vector taking values in the error-set $\mathbb{X}(t) \subset \mathbb{R}^n$ and $\tilde{x}_s(t)$ is a stochastic random vector following the error distribution $p(\tilde{x}_s(t))$.

The challenges addressed in event-based state estimation are as follows:

- Providing *stable* estimation results periodically in time when new measurements are triggered by an event sampling strategy.
- So that stability criteria of the feedback control loop do not depend on the employed sampling strategy, directly.

Such an estimator allows the sensor system to adopt different event sampling strategies depending on, for example, the expected lifetime of its battery. Moreover, a computationally efficient algorithm of the event-based state estimator is desired, to attain applicable solutions.

REMARK 13.1 Stability of estimation results, wherein $\tilde{x}_d$ and $\tilde{x}_s$ denote the estimation errors, implies a nondivergent error-set $\mathbb{X}(t_\mathsf{k})$ and a nondivergent error-covariance $P(t_\mathsf{k})$. More precisely, there exists a constant value for both limits $\lim_{\mathsf{k}\to\infty} \|\mathbb{X}(t_\mathsf{k})\| < \infty$ and $\lim_{\mathsf{k}\to\infty} \lambda_{\max}\big(P(t_\mathsf{k})\big) < \infty$.

After introducing some examples and properties of event-based sampling, the chapter continues with an overview of existing estimators picking either stochastic or deterministic representations for estimating x. In addition, an outlook is presented toward a hybrid state estimator computing the deterministic and the stochastic part of estimation results simultaneously.

13.4 Event-Based Sampling

13.4.1 Illustrative Examples

Event-based sampling is an a-periodic sampling strategy where events are not triggered periodically in time but at instants of predefined events. Three examples are "Send-on-Delta," "Predictive Sampling," and "Matched sampling", as proposed in [3,10,20,22,29]. These strategies define that triggering the next event sample $\mathsf{e} \in \mathbb{Z}_+$ depends on the current measurement $y(t)$ and the previously sampled $y(t_{\mathsf{e}-n})$, for one or more $n \in \mathbb{Z}_{>1}$. More precisely, for some design parameter $\Delta(t)$ and for a predicted measurement value $\hat{y}(t)$, they define the instant of a next event t_e, as follows:

- Send-on-delta:
  $t_\mathsf{e} = \inf\{t > t_{\mathsf{e}-1} \mid \|y(t) - y(t_{\mathsf{e}-1})\| > \Delta(t)\}$.
- Predictive sampling:
  $t_\mathsf{e} = \inf\{t > t_{\mathsf{e}-1} \mid \|y(t) - \hat{y}(t)\| > \Delta(t)\}$.
- Matched sampling:
  $t_\mathsf{e} = \inf\{t > t_{\mathsf{e}-1} \mid D_{\mathrm{KL}}\big(p_1(x(t))||p_2(x(t))\big) > \Delta(t)\}$.

An illustrative impression of the above event sampling strategies is depicted in Figure 13.2. Matched sampling uses the Kullback–Leibler divergence for triggering new events. This divergence, denoted as $D_{\mathrm{KL}}\big(p_1(x)||p_2(x)\big) \in \mathbb{R}_+$, is a *nonsymmetric* measure for the difference of $p_2(x)$ relative to $p_1(x)$. Therein, $p_1(x)$ is considered to be the *updated* (true) PDF of x and $p_2(x)$ is a *prediction* (model) of $p_1(x)$. In line with this reasoning, let $p_2(x(t))$ denote the prediction of $x(t)$ based on the results at $t_{\mathsf{e}-1}$, while $p_1(x(t))$ is the update of $p_2(x(t))$ with the sensor value $y(t)$. Then, their Kullback–Leibler divergence can be regarded as a measure for the relevance of $y(t)$ to the estimation results.

REMARK 13.2 Let the estimation result at $t_{\mathsf{e}-1}$ be the Gaussian $p(x(t_{\mathsf{e}-1})) = \mathcal{G}\big(x(t_{\mathsf{e}-1}), \hat{x}(t_{\mathsf{e}-1}), P(t_{\mathsf{e}-1})\big)$. Further, let the Kullback–Leibler divergence $D_{KL}\big(p_1(x(t))\|p_2(x(t))\big)$ correspond to $p_1(x(t)) = \mathcal{G}\big(x(t), \hat{x}_1(t), P_1(t)\big)$ and $p_2(x(t)) = \mathcal{G}\big(x(t), \hat{x}_2(t), P_2(t)\big)$. Then, the prediction $p_2(x(t))$ and the update $p_1(x(t))$ can be determined with the process model of (13.1) and an a-periodic Kalman filter, that is,

$$\begin{aligned}
P_2(t) &= A_\tau P(t_{\mathsf{e}-1}) A_\tau^\top + B_\tau \mathrm{cov}(w_s(t)) B_\tau^\top; \\
\hat{x}_2(t) &= A_\tau \hat{x}(t_{\mathsf{e}-1}); \\
P_1(t) &= \Big(P_2^{-1}(t) + C^\top \big(\mathrm{cov}(v_s(t))\big)^{-1} C\Big)^{-1}; \\
\hat{x}_1(t) &= P_1^{-1}(t) \Big(P_2^{-1}(t)\hat{x}_2(t) + C^\top \big(\mathrm{cov}(v_s(t))\big)^{-1} y(t)\Big).
\end{aligned}$$

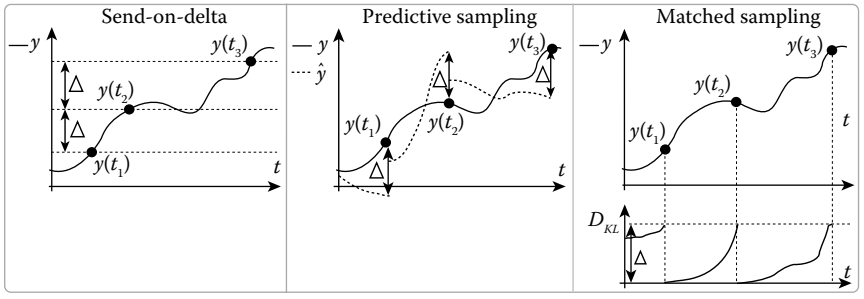

FIGURE 13.2

Illustrative impression for triggering event samples via send-on-delta, predictive sampling, and matched sampling. The latter one employs a Kullback–Leibler divergence denoted as D_{KL}.

Furthermore, the Kullback–Leibler divergence then yields:

$$\begin{aligned} &D_{\mathrm{KL}}\big(p_1(x(t))||p_2(x(t))\big) \\ &\quad := \frac{1}{2}\Big(\log|P_2(t)|\,|P_1(t)|^{-1} + \mathrm{tr}\left(P_2^{-1}(t)P_1(t)\right) - n\Big) \\ &\qquad + \frac{1}{2}\Big(\hat{x}_1(t) - \hat{x}_2(t)\Big)^{\top} P_2^{-1}(t)\big(\hat{x}_1(t) - \hat{x}_2(t)\Big). \end{aligned}$$

The above examples will be used to derive a property of event sampling that shall be exploited in several estimation approaches presented later.

13.4.2 A Sensor Value Property

As new measurement samples are triggered at the instants of well-designed events, not receiving a new measurement sample at the estimator implies that no event has been triggered.* Note that this situation still contains valuable information on the sensor value, as is derived, next.

It was already shown in [30] that the triggering criteria for many of the existing event sampling approaches can be generalized into a set-criteria. To that extent, let us introduce $\mathbb{H}(\mathsf{e},t) \subset \mathbb{R}^m$ as a set in the measurement space collecting all the sensor values that $y(t)$ is allowed to take so that no event will be triggered. Then, a generalization of event sampling has the following definition for triggering a next event t_{e}, that is,

$$t_{\mathsf{e}} = \min\left\{t > t_{\mathsf{e}-1} | y(t) \notin \mathbb{H}(\mathsf{e},t)\right\}. \tag{13.3}$$

Then, the sensor value property derived from the above generalization yields

Proposition 13.1

Let $y(t)$ be sampled with an event strategy similar to (13.3). Then, $y(t) \in \mathbb{H}(\mathsf{e},t)$ holds for any $t \in [t_{\mathsf{e}-1}, t_{\mathsf{e}})$.

*Under the assumption that no package loss can occur.

With send-on-delta, the triggering set $\mathbb{H}(\mathsf{e},t)$ is an m-dimensional ball of radius Δ centered at $y(t_{\mathsf{e}-1})$, for all $t_{\mathsf{e}-1} < t < t_{\mathsf{e}}$, while for predictive sampling the triggering set $\mathbb{H}(\mathsf{e},t)$ is the same ball but then centered at $\hat{y}(t)$. Similarly, the triggering set $\mathbb{H}(\mathsf{e},t)$ for matched sampling is the ellipsoidal shaped set $\mathbb{H}(\mathsf{e},t) = \mathbb{L}_{(\mu(t),\Sigma(t))}$. Values for the center $\mu(t) \in \mathbb{R}^m$ and covariance $\Sigma(t) \in \mathbb{R}^{m\times m}$ defining the boundary of the ellipsoid are found in [20].

Proposition 13.1 formalizes the inherent measurement knowledge of event sampling, that is, *not* receiving a new measurement for any $t \in [t_{\mathsf{e}-1}, t_{\mathsf{e}})$ implies that $y(t)$ is included in $\mathbb{H}(\mathsf{e},t)$. A characterization of $\mathbb{H}(\mathsf{e},t)$ can be derived prior to the event instant t_{e} as the triggering condition is available. It is exactly this set-membership property of event sampling that gives the additional measurement information for updating estimation results.

13.5 Existing State Estimators

The challenge in event-based state estimation is an unknown time horizon until the next event occurs, if it even occurs at all. Solutions with a-periodic estimators, for example, [4,19,35], perform a prediction of the state x periodically in time when no measurement is received. It was shown in [31] that this leads to a diverging behavior of the error-covariance $\mathrm{cov}(\tilde{x}_s)$ (unless the triggering condition depends on the error-covariance, as it is shown in [34–36]). The diverging property was proven by assuming Gaussian noise representation and no deterministic noises or state-error representations, that is, $\mathbb{W} = \emptyset$, $\mathbb{V} = \emptyset$, and $\mathbb{X} = \emptyset$. To curtail the runaway error-covariance, some alternative a-periodic estimators were proposed in [13,17] focusing on *when* to send new measurements so to minimize estimation error. Criteria developed for sending a new measurement are set to guarantee stability, implying that

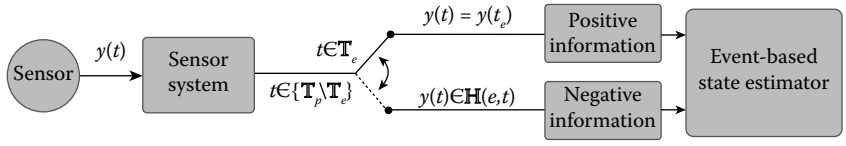

FIGURE 13.3

Illustrative setup of a typical event-based state estimator: a new measurement sample $y(t) = y(t_\mathsf{e})$ arrives at the instants of an event $t \in \mathbb{T}_e$, while the measurement information $y(t) \in \mathbb{H}(\mathsf{e}, t)$ is implied periodically in time when no event occurs at $t \in \{\mathbb{T}_p \setminus \mathbb{T}_e\}$.

the stability of these estimators directly depends on the employed event triggering condition.

In the considered problem, a sensor is not limited to one event sampling strategy but employed strategies can be replaced depending on the situation at hand. Therefore, guaranteeing stable estimation results under these circumstances calls for a redesign of existing estimators. Key in this redesign is the additional knowledge on the sensor value that becomes available when no new measurement was sampled, that is, Proposition 13.1. An early solution able to exploit this idea was proposed in [25], where the results of Proposition 13.1 are used to perform a state update periodically in time when no event was triggered. However, the setup therein is restricted to the sampling strategy "send-on-delta" and no proof of stability was derived. The remaining three estimators of this overview do give a proof of stability and are not restricted to one specific event sampling strategy.

An overall summary of the three estimation approaches is presented, first, before continuing with more details per approach. Assumptions on the characterization of process noise, measurement noise and estimation results, that is, purely stochastic, purely deterministic or a combination of the two, form the basis for distinguishing the three event-based estimation approaches. Apart from that, all three approaches have an estimation setup as it is depicted in Figure 13.3. The estimator is able to exploit measurements from any event sampling strategy, so that updated estimation results are computed at least periodically in time. An aspect that differs is that the deterministic estimation approach checks the event criteria periodically in time, implying that $\mathbb{T}_e \subset \mathbb{T}_p$ and allowing the deterministic estimator to run periodically as well. With the stochastic and the combined estimation approaches, the event instants can occur at any time, implying that $\mathbb{T}_e$ and $\mathbb{T}_p$ will have (almost) no overlapping time instants enforcing these two estimators to run at both types of instants, that is, $\mathbb{T}_e \cap \mathbb{T}_p$. The main challenge in all three estimators is to cope with the hybrid nature of measurement information available:

- Positive information: At the instants $t \in \mathbb{T}_e$ of an event, a new measurement value $y(t) = y(t_\mathsf{e})$ is received.
- Negative information: At time-periodic instants $t \in \{\mathbb{T}_p \setminus \mathbb{T}_e\}$ that are not an event, the measurement information is a property that the sensor value lies within a bounded subset, that is, $y(t) \in \mathbb{H}(\mathsf{e}, t)$.

13.5.1 Stochastic Representations

This section summarizes the *stochastic* event-based state estimator (*s*EBSE) originally developed in [30] and later applied for a target tracking application in videos in [24]. The estimator was further extended in [28] toward multiple sensor systems each having their own triggering criteria. As mentioned, the *s*EBSE computes updated estimation results at both event and periodic instants, that is, for all $t_\mathsf{k} \in \mathbb{T} = \mathbb{T}_e \cup \mathbb{T}_p$. It is important to note that the *s*EBSE proposed in [30] does not consider deterministic noises or state errors, that is, $\mathbb{W}$, $\mathbb{V}$, and $\mathbb{X}$ are empty sets. Further, the stochastic process and measurement noise are Gaussian distributed*:

$$w_s(t_\mathsf{k}) \sim \mathcal{G}(0, W) \quad \text{and} \quad v_s(t_\mathsf{k}) \sim \mathcal{G}(0, V), \quad \forall t_k \in \mathbb{T}. \tag{13.4}$$

Similarly, the estimation result $x(t_\mathsf{k}) = \hat{x}(t_\mathsf{k}) + \tilde{x}_s(t_\mathsf{k})$ of this estimator is Gaussian as well, where $\hat{x}(t_\mathsf{k})$ is the estimated mean and the error-covariance $P(t_\mathsf{k}) \in \mathbb{R}^{n \times n}$ characterizes $\tilde{x}_s(t_\mathsf{k}) \sim \mathcal{G}(0, P(t_\mathsf{k}))$. Explicit formulas for finding an approximation of $\hat{x}(t_\mathsf{k})$ and $P(t_\mathsf{k})$ are summarized next.

Let us assume that $\mathsf{e} - 1$ events were triggered until t_k. Then, the new measurement information at t_k is either the received measurement value $y(t_\mathsf{k}) = y(t_\mathsf{e})$, when $t_\mathsf{k} \in \mathbb{T}_e$ is an *event* instant, or it is the inherent knowledge that $y(t_\mathsf{k}) \in \mathbb{H}(\mathsf{e}, t_\mathsf{k})$, when $t_\mathsf{k} \in \{\mathbb{T}_p \setminus \mathbb{T}_e\}$ is not an event but a time-periodic instant. This measurement information can be rewritten by introducing the bounded Borel set $\mathbb{Y}(t_\mathsf{k}) \in \mathbb{R}^m$ as follows:

$$\begin{aligned} \mathbb{Y}(t_\mathsf{k}) &:= \begin{cases} \mathbb{H}(\mathsf{e}, t_\mathsf{k}) & \text{if} \quad t_\mathsf{k} \in \{\mathbb{T}_p \setminus \mathbb{T}_e\}, \\ \{y(t_\mathsf{e})\} & \text{if} \quad t_\mathsf{k} \in \mathbb{T}_e. \end{cases} \\ &\Rightarrow \quad y(t_\mathsf{k}) \in \mathbb{Y}(t_\mathsf{k}), \ \forall t_\mathsf{k} \in \mathbb{T}. \end{aligned} \tag{13.5}$$

With the above result one can derive that the PDF of $x(t_\mathsf{k})$, as it is to be determined by this *s*EBSE,

*Recall that $x \sim \mathcal{G}(\mu, \Sigma)$ is a short notation for $p(x) = \mathcal{G}(x, \mu, \Sigma)$.

yields $p\big(x(t_k)|y(t_0)\in\mathbb{Y}(t_0),\ldots,y(t_k)\in\mathbb{Y}(t_k)\big)$, which is denoted as $p\big(x(t_k)|\mathbb{Y}(t_{0:k})\big)$ for brevity. An exact solution for this PDF is found by applying Bayes' rule, see [21] for more details, that is,

$$p\big(x(t_k)|\mathbb{Y}(t_{0:k})\big) = \frac{p\left(x(t_k)\middle|\mathbb{Y}(t_{0:k-1})\right)p\big(y(t_k)\in\mathbb{Y}(t_k)|x(t_k)\big)}{\int_{\mathbb{R}^n} p\left(x(t_k)\middle|\mathbb{Y}(t_{0:k-1})\right)p\big(y(t_k)\in\mathbb{Y}(t_k)|x(t_k)\big)\mathrm{d}x(t_k)}. \tag{13.6}$$

The *s*EBSE developed in [30] finds an single Gaussian approximation of the above equation in three steps.

Step 1 Compute the *prediction* $p\big(x(t_k)|\mathbb{Y}(t_{0:k-1})\big)$ of (13.6) from the process model in (13.1) and the estimation result at t_{k-1}, that is, $p\big(x(t_{k-1})|\mathbb{Y}(t_{0:k-1})\big)$. Note that the process model is linear and that $p\big(x(t_{k-1})|\mathbb{Y}(t_{0:k-1})\big)\approx\mathcal{G}\big(x(t_{k-1}),\hat{x}(t_{k-1}),P(t_{k-1})\big)$ is Gaussian. Hence, standard (a-periodic) Kalman filtering equations can be used to find the *predicted* PDF $p\big(x(t_k)|\mathbb{Y}(t_{0:k-1})\big)$, for some sampling time $\tau_k := t_k - t_{k-1}$, that is*,

$$p\big(x(t_k)|\mathbb{Y}(t_{0:k-1})\big) := \mathcal{G}\big(x(t_k),\hat{x}(t_k^-),P(t_k^-)\big), \tag{13.7}$$

where,

$$\begin{aligned}\hat{x}(t_k^-) &:= A_{\tau_k}\hat{x}(t_{k-1}),\\ P(t_k^-) &:= A_{\tau_k}P(t_{k-1})A_{\tau_k}^\top + B_{\tau_k}WB_{\tau_k}^\top;\end{aligned}$$

Step 2 Formulate the *likelihood* $p\big(y(t_k)\in\mathbb{Y}(t_k)|x(t_k)\big)$ as a summation of N Gaussians and employ a sum-of-Gaussian approach proposed in [32] to solve $p\big(x(t_k)|\mathbb{Y}(t_{0:k})\big)$ in (13.6). More details on this likelihood are presented later but, for now, let us point out that this solution will result in a summation of N Gaussians characterized by N normalized weights $\alpha_q\in\mathbb{R}_+$, N means $\hat{\theta}_q\in\mathbb{R}^n$, and N covariances $\Theta_q\in\mathbb{R}^{n\times n}$:

$$p\big(x(t_k)|\mathbb{Y}(t_{0:k})\big)\approx\sum_{q\in\mathbb{Z}_{[1,N]}}\alpha_q(t_k)\mathcal{G}\big(x(t_k),\hat{\theta}_q(t_k),\Theta(t_k)\big). \tag{13.8}$$

The variables of this formula have the following expression:

$$\begin{aligned}\Theta(t_k) &= \big(P^{-1}(t_k^-)+C^\top R^{-1}(t_k)C\big)^{-1},\\ \hat{\theta}_q(t_k) &= \Theta(t_k)\big(P^{-1}(t_k^-)\hat{x}(t_k^-)+C^\top R^{-1}(t_k)\hat{y}_q(t_k)\big),\\ \omega_q(t_k) &= e^{\left(\hat{y}_q(t_k)-C\hat{x}(t_k^-)\right)^\top\left(CP(t_k^-)C^\top+R(t_k)\right)^{-1}\left(\hat{y}_q(t_k)-C\hat{x}(t_k^-)\right)},\\ \alpha_q(t_k) &= \omega_q(t_k)\left(\sum_{q\in\mathbb{Z}_{[1,N]}}\omega_q(t_k)\right)^{-1}.\end{aligned}$$

Herein, $\omega_q(t_k)\in\mathbb{R}_+$, $\hat{y}_q(t_k)\in\mathbb{R}^m$, and $R(t_k)\in\mathbb{R}^{m\times m}$ are obtained from the likelihood function, which is modeled with the following weighted summation of N Gaussian:

$$p\left(y(t_k)\in\mathbb{Y}(t_k)\middle|x(t_k)\right)\approx\sum_{q\in\mathbb{Z}_{[1,N]}}\omega_q(t_k)\mathcal{G}\big(\hat{y}_q(t_k),Cx(t_k),R(t_k)\big). \tag{13.9}$$

Step 3 Approximate the result of Step 2 from a sum of N Gaussians into the desired single Gaussian $p(x(t_k))=\mathcal{G}\big(x(t_k),\hat{x}(t_k)P(t_k)\big)$. The mean $\hat{x}(t_k)$ and error-covariance $P(t_k)$ should correspond to the mean and covariance of $p\big(x(t_k)|\mathbb{Y}(t_{0:k})\big)$ in (13.8), yielding

$$\hat{x}(t_k)=\sum_{q\in\mathbb{Z}_{[1,N]}}\alpha_q(t_k)\hat{\theta}_q(t_k),$$

and

$$P(t_k)=\sum_{q\in\mathbb{Z}_{[1,N]}}\alpha_q(t_k)\Big(\Theta(t_k)+\big(\hat{x}(t_k)-\hat{\theta}_q(t_k)\big)\times\big(\hat{x}(t_k)-\hat{\theta}_q(t_k)\big)^\top\Big).$$

Stability of the above stochastic estimator *s*EBSE has been derived in [30].

Theorem 13.1

Let $\mathbb{H}(\mathsf{e}|t_k)$ be a given bounded Borel set for all $k\in\mathbb{Z}_+$ and let (A_{τ_s},C) be an observable pair. Then, the s*EBSE* results in a stable estimate, that is, $\lim_{k\to\infty}\lambda_{\max}(P(t_k))$ exists and is bounded.

A key aspect of the *s*EBSE is to turn the set inclusion $y(t_k)\in\mathbb{H}(\mathsf{e},t_k)$ into a stochastic likelihood characterized by N Gaussians (see Equation 13.9). Open questions on how to come up with such a characterization are discussed in the next example and finalizes the *s*EBSE.

EXAMPLE 13.1: From set inclusion to likelihood This example finds a solution for the likelihood $p\left(y(t_k)\in\mathbb{Y}(t_k)\middle|x(t_k)\right)$ in (13.9) by starting from the inclusion $y(t_k)\in\mathbb{Y}(t_k)$. Normally, that is, when $y(t_k)$ is an actual measurement, a likelihood is of the form $p(y(t_k)|x(t_k))$. The process model in (13.2) together with

*The notation t_k^- is used to emphasize the predictive character of a variable at t_k.

the noise assumptions on v_d and v_s in (13.4) then give that such a standard likelihood is Gaussian, that is,

$$p\big(y(t_\mathsf{k})\big|x(t_\mathsf{k})\big) = G\big(y(t_\mathsf{k}), Cx(t_\mathsf{k}), V\big). \tag{13.10}$$

In the above estimator, $y(t_\mathsf{k})$ has been generalized into a set inclusion $y(t_\mathsf{k}) \in \mathbb{Y}(t_\mathsf{k})$, which can be regarded as a quantized measurement. Results in [18] point out that the corresponding likelihood of this inclusion is found by a convolution of $p\big(y(t_\mathsf{k})\big|x(t_\mathsf{k})\big)$ in (13.10) for all possible measurement values $y(t_\mathsf{k}) \in \mathbb{Y}(t_\mathsf{k})$. In a fully stochastic description, this is similar to a convolution of the PDF in (13.10) with a uniform PDF $p_{\mathbb{Y}(t_\mathsf{k})}\big(y(t_\mathsf{k})\big)$ being constant (> 0) for all $y(t_\mathsf{k}) \in \mathbb{Y}(t_\mathsf{k})$ and 0 otherwise. The likelihood of such a quantized measurement $y(t_\mathsf{k}) \in \mathbb{Y}(t_\mathsf{k})$ is then found via

$$\begin{aligned} &p\big(y(t_\mathsf{k}) \in \mathbb{Y}(t_\mathsf{k})\big|x(t_\mathsf{k})\big) \\ &\quad = \int_{\mathbb{R}^m} p\big(y(t_\mathsf{k})\big|x(t_\mathsf{k})\big)\, p_{\mathbb{Y}(t_\mathsf{k})}\big(y(t_\mathsf{k})\big)\mathrm{d}y(t_\mathsf{k}). \end{aligned} \tag{13.11}$$

This uniform PDF has a hybrid expression in line with $\mathbb{Y}(t_\mathsf{k})$ in (13.5). At instants of an event, the set is the actual measurement $\mathbb{Y}(t_\mathsf{k}) := \{y(t_\mathsf{e})\}$ and the PDF $p_{\mathbb{Y}(t_\mathsf{k})}\big(y(t_\mathsf{k})\big)$ is described with a delta function at $y(t_\mathsf{e})$. Periodically in time, the set is defined by the triggering criteria $\mathbb{Y}(t_\mathsf{k}) = \mathbb{H}(\mathsf{e}, t_\mathsf{k})$ at which $p_{\mathbb{Y}(t_\mathsf{k})}\big(y(t_\mathsf{k})\big)$ will be approximated by a summation of N Gaussians. As such, the following characterization is introduced:

$$\begin{aligned} &p_{\mathbb{Y}(t_\mathsf{k})}\big(y(t_\mathsf{k})\big) \\ &\approx \begin{cases} \sum_{q=1}^{N} \frac{1}{N} G\big(y(t_\mathsf{k}), \hat{y}_q(t_\mathsf{k}), U(t_\mathsf{k})\big) & \text{if} \quad t_\mathsf{k} \in \{\mathbb{T}_p \setminus \mathbb{T}_e\}, \\ \delta\big(y(t_\mathsf{k}) - y(t_\mathsf{e})\big) & \text{if} \qquad t_\mathsf{k} \in \mathbb{T}_\mathsf{e}. \end{cases} \end{aligned}$$

Values of $\hat{y}_q(t_\mathsf{k}) \in \mathbb{R}^m$, for all $q \in \mathbb{Z}_{[1,N]}$, are retrieved by taking N equidistant samples in the event triggering set $\mathbb{Y}(t_\mathsf{k}) = \mathbb{H}(\mathsf{e}|t_\mathsf{k})$. Each sample represents the mean of a Gaussian $\mathcal{G}\big(y(t_\mathsf{k}), \hat{y}_q(t_\mathsf{k}), U(t_\mathsf{k})\big)$, where $U \in \mathbb{R}^{m\times m}$ is a constant for each Gaussian (see Figure 13.4).

Then, substituting the above approximation and $p\big(y(t_\mathsf{k})\big|x(t_\mathsf{k})\big)$ of (13.10) into the expression of the "set-inclusion"-likelihood in (13.11) gives a result for $p\big(y(t_\mathsf{k}) \in \mathbb{Y}(t_\mathsf{k})\big|x(t_\mathsf{k})\big)$ already pointed out in (13.9), where

- $N = 1$, $\hat{y}_1(t_\mathsf{k}) = y(t_\mathsf{e})$ and $R(t_\mathsf{k}) = V$ when $t_\mathsf{k} \in \mathbb{T}_e$ is an event.
- $N \geq 1$, $\hat{y}_q(t_\mathsf{k})$ are the equidistantly sampled values of $\mathbb{H}(\mathsf{e}, t_\mathsf{k})$ and $R(t_\mathsf{k}) = U(t_\mathsf{k}) + V$ when $t_\mathsf{k} \in \{\mathbb{T}_p \setminus \mathbb{T}_e\}$ is a periodic instant.

13.5.2 Deterministic Representations

This section reviews the *deterministic* event-based state estimator (*d*EBSE) developed in [27]. The main difference with respect to the previous approach is that the *d*EBSE operates on time-periodic instants only, that is, $t_\mathsf{k} \in \mathbb{T} := \mathbb{T}_p$ and $\mathbb{T}_e \subseteq \mathbb{T}_p$. As such, the sensor value is periodically checked on violation of the event triggering criteria, to generate new measurements. This simplifies the a-periodic process model in (13.1) as the sampling time is the constant τ_s, that is, $\bar{A} := A_{\tau_s}$, $\bar{B} := B_{\tau_s}$, resulting in:

$$x(t_\mathsf{k}) = \bar{A}x(t_{\mathsf{k}-1}) + \bar{B}w(t_{\mathsf{k}-1}); \tag{13.12}$$

$$y(t_\mathsf{k}) = Cx(t_\mathsf{k}) + v(t_\mathsf{k}). \tag{13.13}$$

It is important to note that the *d*EBSE does not assume stochastic noise terms. Further, the deterministic process and measurement noise are in line with the problem formulation presented in Section 13.3:

$$w_d(t_\mathsf{k}) \in \mathbb{W} \quad \text{and} \quad v_d(t_\mathsf{k}) \in \mathbb{V}, \quad \forall t_\mathsf{k} \in \mathbb{T}_p, \tag{13.14}$$

where $\mathbb{W} \subset \mathbb{R}^l$ and $\mathbb{V} \subset \mathbb{R}^m$ are unbiased. In line with these noise representations, the *d*EBSE assumes a deterministic representation of its estimation results, that is, $\tilde{x}_s(t_\mathsf{k}) = 0$ for all $t_\mathsf{k} \in \mathbb{T}$. The deterministic estimation

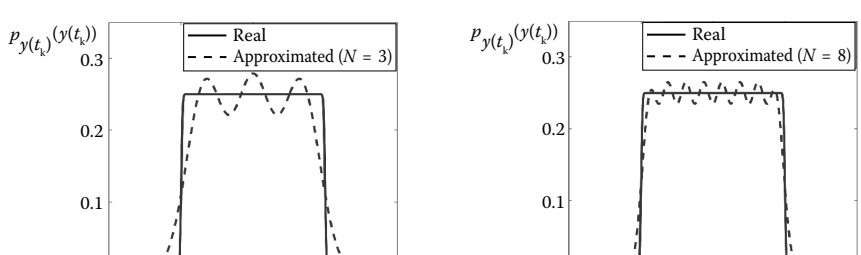

FIGURE 13.4

Two approximations of the uniform PDF $p_{[-2,2]}\big(y(t_\mathsf{k})\big)$ by a summation of either 3 or 8 Gaussians having equidistantly sampled means regarding their measurement value $\hat{y}_q(t_\mathsf{k})$. The covariance matrix $U(t_\mathsf{k})$ of each individual Gaussian function is computed with the heuristic expression $U(t_\mathsf{k}) = c\Big(0.25 - 0.05e^{-\frac{4(N-1)}{15}} - 0.08e^{-\frac{4(N-1)}{180}}\Big)$, where the positive scalar c is equal to the Eucledian distance between two neighboring means.

error is approximated as a circular set based on some p-norm, that is,

$$\|\hat{x}(t_k) - x(t_k)\|_p \leq \gamma(t_k), \ \ \forall t_k \in \mathbb{T}_p \text{ and some } \gamma(t_k) > 0.$$

The event triggering criteria presented next follows a similar approach, for which it is assumed that $e - 1$ events were triggered until t_k. Then, for some known measurement value $\hat{y}^{cond}$ conditioned on the prior estimation result, the event triggering criteria of the dEBSE adopt a p-norm criteria, that is,

$$\begin{aligned} &\textit{an} \text{ event is triggered at } t_k \text{ if} \quad \|y(t_k) - \hat{y}^{cond}(t_k)\|_p > \Delta, \\ &\textit{no} \text{ event is triggered at } t_k \text{ if} \quad \|y(t_k) - \hat{y}^{cond}(t_k)\|_p \leq \Delta. \end{aligned}$$

The new measurement information at t_k, which is denoted with the implied measurement $z(t_k)$, is either the received measurement $y(t_k)$, when $t_k \in \mathbb{T}_e$ is an *event* instant, or it is the knowledge that $\|y(t_k) - \hat{y}^{cond}(t_k)\|_p \leq \Delta$, when $t_k \in \{\mathbb{T}_p \setminus \mathbb{T}_e\}$ is not an event instant. The latter measurement information is treated as a measurement realization via $z(t_k) = \hat{y}^{cond}(t_k) + \delta(t_k)$, where $\delta(t_k)$ is bounded by a circular set of known radius.

The implied measurement values $z(t_k)$ available at any sample instant $t_k \in \mathbb{T}$ are used to compute updated values of the estimated mean $\hat{x}(t_k)$. A value for the error bound $\gamma(t_k)$ is not actively tracked. Instead, it is proven that there exists a bound on $\gamma(t_k)$ for all $t_k \in \mathbb{T}$. Yet, before presenting this bound, let us start with the estimation procedure adopted by the dEBSE, which is based on the moving horizon approach presented in [2].

This moving horizon approach focuses on estimating the state at t_{k-N} given all measurements from the current time instant t_k until t_{k-N}.* As such, the method focuses on estimating $\hat{x}(t_{k-N})$ given $z(t_{k-N:k})$. The estimation result at the current instant t_k is then a forward prediction of $\hat{x}(t_{k-N})$. Let us denote this forward prediction as $\hat{x}^-(t_k)$, to point out that it is still a prediction which will receive its final estimation result at t_{k+N}. Then, the forward prediction yields

$$\hat{x}^-(t_k) = A^N \hat{x}(t_{k-N}).$$

A solution for computing $\hat{x}(t_{k-N})$ requires the selection of several design parameters, such as $\alpha \in \mathbb{R}_+$ and $W_N \in \mathbb{R}^{n \times Nm}$. Then, the estimated mean $\hat{x}(t_{k-N})$ based on its prior result $\hat{x}(t_{k-N-1})$ yields

$$\begin{aligned} \hat{x}(t_{k-N}) = &\left(\alpha I + K_N^\top K_N\right) \\ &\times \left(\alpha \bar{A} x(t_{k-N-1}) + O_N^\top W_N \begin{pmatrix} z(t_{k-N}) \\ \vdots \\ z(t_k) \end{pmatrix}\right), \end{aligned} \tag{13.15}$$

where

$$K_N = W_N \begin{pmatrix} C & C\bar{A} & \cdots & C\bar{A}^{N+1} \end{pmatrix}^\top. \tag{13.16}$$

The employed values for α and W_N are an indication of the confidence in measurements. A suitable value for W_N depending on a positive scalar β is found via a singular value decomposition of the observability matrix $VSU^\top := \begin{pmatrix} C & CA & \cdots & CA^{N+1} \end{pmatrix}^\top$. Then, since some singular values are likely zero, one can construct a weighted "pseudo-inverse" of this observability matrix, that is,

$$W_N = \sqrt{\beta} V S^+ U^\top. \tag{13.17}$$

The advantage of the above weight matrix selection is that $K_N = \begin{pmatrix} 0 I_{n_1} & 0 \\ 0\sqrt{\beta} & I_{n_2} \end{pmatrix}$, where n_1 is the number of unobservable state elements and $n_2 := n - n_1$ is the number of observable state elements. With this result one can make the following generalization, which is instrumental for the stability result presented afterwards:

$$\left(\alpha I + K_N^\top K_N\right) \alpha \bar{A} = \begin{pmatrix} \bar{A}_{11} & \bar{A}_{12} \\ 0 & \frac{\alpha}{\alpha+\beta} \bar{A}_{22} \end{pmatrix}.$$

Theorem 13.2

Let the pair $(\bar{A}, C)$ be detectable, let W_N follow (13.17), and let $\alpha > 0$ and β be chosen such that $|\lambda_{\max}\left(\alpha(\alpha+\beta)^{-1}\bar{A}_{22}\right)| < 1$. Then, the dEBSE is a stable observer for the process in (13.12), that is, $\|\hat{x}(t_k) - x(t_k)\| < \epsilon$ for all $t_k \in \mathbb{T}_p$ if $\|\hat{x}(t_0) - x(t_0)\| < \eta$, for some bounded $\epsilon, \eta > 0$.

A proof of the above theorem is found in [27].

Note that the estimators in this section either address stochastic or deterministic weights. Yet, more realistic scenarios favor estimators that can address both types of noises. In most practical cases, the process and measurement noise are represented by Gaussian distributions with no deterministic part. Yet, the implied measurement information when exploiting event sampling strategies is typically modeled as additive deterministic noise on the sensor measurement y. An estimator able to cope with both types of noise representations is proposed in the next section.

*For clarity of expression, details on the estimation approach directly after initialization and until the Nth sample instant are not presented. The interested reader is referred to [27] for more details.

13.6 A Hybrid State Estimator

This section presents a *hybrid* event-based state estimator (*h*EBSE) allowing both *stochastic* and *deterministic* representations of noise and estimation results. Yet, for clarity of exposition, the presented estimator does not consider deterministic process noises, that is, $\mathbb{W} = \emptyset$. The *h*EBSE is based on existing estimators combining stochastic and deterministic measurement noises, as they were proposed in [26] and to some extent in [11]. In line with the previous *s*EBSE, updated estimation results are computed at both event instants as well as at periodic instants, that is, for all $t_\mathsf{k} \in \mathbb{T} = \mathbb{T}_e \cup \mathbb{T}_s$. It is important to note that the proposed estimator assumes a Gaussian distribution of the stochastic noises and an ellipsoidal set inclusion for the deterministic noise parts.* More precisely, let us introduce the following noise characteristics in line with the problem formulation of Section 13.3:

$$\begin{aligned} &w_s(t_\mathsf{k}) \sim \mathcal{G}(0, W),\ v_d(t_\mathsf{k}) \in \mathbb{L}_{0,D} \ \text{ and} \\ &v_s(t_\mathsf{k}) \sim \mathcal{G}(0, V), \quad \forall t_\mathsf{k} \in \mathbb{T}. \end{aligned} \tag{13.18}$$

Herein, $W \in \mathbb{R}^{l\times l}$ is a positive definite matrix characterizing process noise, while $D, V \in \mathbb{R}^{m\times m}$ are positive definite matrices defining the ellipsoidal shaped set $\mathbb{L}_{0,D}$ and the Gaussian function $\mathcal{G}(0, V)$ for characterizing measurement noise. The *h*EBSE further defines $\mathrm{t}x(t_\mathsf{k}) = \hat{x}(t_\mathsf{k}) + \tilde{x}_d(t_\mathsf{k}) + \tilde{x}_s(t_\mathsf{k})$ for representing its estimation results, consisting of a stochastic and a deterministic part as introduced in Section 13.3. The estimation result has a mean $\hat{x}(t_\mathsf{k})$ and its estimation errors are characterized as follows:

$$\tilde{x}_d(t_\mathsf{k}) \in \mathbb{L}_{0,X(t_\mathsf{k})}, \quad \tilde{x}_s(t_\mathsf{k}) \sim \mathcal{G}(0, P(t_\mathsf{k})), \quad \forall t_\mathsf{k} \in \mathbb{T}. \tag{13.19}$$

Herein, $X, P \in \mathbb{R}^{n\times n}$ are positive definite matrices defining the ellipsoidal shaped set $\mathbb{L}_{0,X(t_\mathsf{k})}$ and the Gaussian $\mathcal{G}(0, P(t_\mathsf{k}))$, respectively.

REMARK 13.3 The matrices D and $X(t_\mathsf{k})$ are referred to as shape matrices, whereas W, V, and $P(t_\mathsf{k})$ are covariance matrices. Moreover, since $\tilde{x}_d$ and $\tilde{x}_s$ denote an estimation error, let us refer to $X(t_\mathsf{k})$ and $P(t_\mathsf{k})$ as the error-shape matrix and the error-covariance matrix, respectively.

Explicit formulas for finding values of $\hat{x}(t_\mathsf{k})$, $P(t_\mathsf{k})$, and $X(t_\mathsf{k})$ are presented, next. To that extent, it is assumed that the process model in (13.1) is available, along with the values for W, V, and D. The proposed *h*EBSE is presented in two stages. Firstly, the implied measurement information resulting from event triggering criteria is integrated with the deterministic part of the measurement noise v_d. Secondly, the state estimation formulas of the *h*EBSE are presented, which are based on the combined stochastic and set-membership estimator proposed in [26].

*Recall that $x \sim \mathcal{G}(\mu, \Sigma)$ is a short notation for $p(x) = \mathcal{G}(x, \mu, \Sigma)$ and that $\mathbb{L}_{\mu,\Sigma}\mathbb{R}^q$ is an ellipsoidal shaped set defined by $\mathbb{L}_{\mu,\Sigma} := \{x \in \mathbb{R}^q | (x-\mu)^\top \Sigma^{-1}(x-\mu) \le 1\}$.

13.6.1 Implied Measurements

The measurement information available at any sample instant, that is, event or time-periodic, has already been derived in Sections 13.4.2 and 13.5.1. To summarize those results, let us assume that $\mathsf{e}-1$ event were triggered until t_k. Then, the measurement information at t_k is either a received measurement value $y(t_\mathsf{k}) = y(t_\mathsf{e})$, when $t_\mathsf{k} \in \mathbb{T}_e$ is an *event* instant, or it is a set-inclusion $y(t_\mathsf{k}) \in \mathbb{H}(\mathsf{e}, t_\mathsf{k})$, when $t_\mathsf{k} \in \mathbb{T}_p \setminus \mathbb{T}_e$ is not an event but a time-periodic instant. This measurement information can be rewritten as follows:

$$y(t_\mathsf{k}) \in \begin{cases} \mathbb{H}(\mathsf{e}, t_\mathsf{k}) & \text{if} \quad t_\mathsf{k} \in \mathbb{T}_p \setminus \mathbb{T}_e, \\ \{y(t_\mathsf{e})\} & \text{if} \quad t_\mathsf{k} \in \mathbb{T}_e. \end{cases} \tag{13.20}$$

Now, let us assume that the event triggering set $\mathbb{H}(\mathsf{e}, t_\mathsf{k})$ is (or can be approximated by) the ellipsoidal set $\mathbb{L}_{(\hat{y}_\mathsf{e}(t_\mathsf{k}), H_\mathsf{e}(t_\mathsf{k}))}$, for example,

$$\begin{aligned} &[\hat{y}_\mathsf{e}(t_\mathsf{k}),\, H_\mathsf{e}(t_\mathsf{k})] := \arg \min_{\hat{y}\in\mathbb{R}^m,\, H\succeq 0} \quad \mathrm{tr}(H), \\ &\text{subject to:} \qquad \mathbb{L}_{(\hat{y},H)} \supseteq \mathbb{H}(\mathsf{e}, t_\mathsf{k}). \end{aligned} \tag{13.21}$$

Similarly, the remaining set $\{y(t_\mathsf{e})\}$ of the measurement information in (13.20) can be approximated by the ellipsoidal set $\lim_{\epsilon\downarrow 0} \mathbb{L}_{(y(t_\mathsf{e}),\epsilon I)}$. Substituting these values into (13.20) and considering $\epsilon \downarrow 0$ gives

$$y(t_\mathsf{k}) \in \begin{cases} \mathbb{L}_{(\hat{y}_\mathsf{e}(t_\mathsf{k}), H_\mathsf{e}(t_\mathsf{k}))} & \text{if} \quad t_\mathsf{k} \in \mathbb{T}_p \setminus \mathbb{T}_e, \\ \mathbb{L}_{(y(t_\mathsf{e}),\epsilon I)} & \text{if} \quad t_\mathsf{k} \in \mathbb{T}_e. \end{cases}$$

One can turn the above set-membership into an equality by introducing the unbiased noise term $e(t_\mathsf{k})$, such that $e(t_\mathsf{k}) \in \mathbb{L}_{(0,H_\mathsf{e}(t_\mathsf{k}))}$ if $t_\mathsf{k} \in \mathbb{T}_p \setminus \mathbb{T}_e$ and $e(t_\mathsf{k}) \in \mathbb{L}_{(0,\epsilon I)}$ if $t_\mathsf{k} \in \mathbb{T}_e$, resulting in the realization

$$y(t_\mathsf{k}) + e(t_\mathsf{k}) = \begin{cases} \hat{y}_\mathsf{e}(t_\mathsf{k}) & \text{if} \quad t_\mathsf{k} \in \mathbb{T}_p \setminus \mathbb{T}_e, \\ y(t_\mathsf{e}) & \text{if} \quad t_\mathsf{k} \in \mathbb{T}_e. \end{cases} \tag{13.22}$$

Since $y(t_\mathsf{k}) = Cx(t_\mathsf{k}) + v_s(t_\mathsf{k}) + v_d(t_\mathsf{k})$ already contains a deterministic noise term $v_d \in \mathbb{L}_{(0,D)}$, one can introduce $\tilde{v}(d)(t_\mathsf{k}) := v_d(t_\mathsf{k}) + e(t_\mathsf{k})$ satisfying the following set-inclusion, for some $\varsigma \in (0, 1)$, that is,

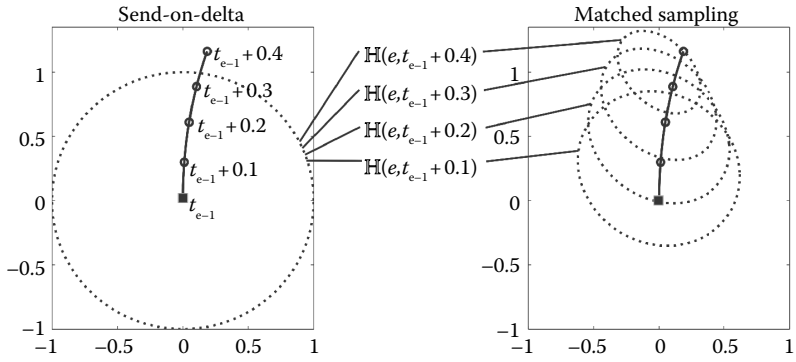

FIGURE 13.5

Illustrative examples of the event triggering sets $\mathbb{H}(\mathsf{e},t) \in \mathbb{R}^2$ that result from send-on-delta and matched sampling for the periodic sample instants $t_{\mathsf{e}-1}+0.1$ until $t_{\mathsf{e}-1}+0.4$ seconds. The initial measurement value is $y(t_{\mathsf{e}-1}) = (0\ 0)^\top$ for both strategies.

$\tilde{v}_d(t_\mathsf{k})$

$$\in \begin{cases} \mathbb{L}_{(0,D)} \oplus \mathbb{L}_{(0,H_\mathsf{e}(t_\mathsf{k}))} \\ \quad \subseteq \mathbb{L}_{\left(0,(1+\varsigma^{-1})D+(1+\varsigma)H_\mathsf{e}(t_\mathsf{k})\right)} & \text{if} \quad t_\mathsf{k} \in \mathbb{T}_p \setminus \mathbb{T}_e, \\ \mathbb{L}_{(0,D)} \oplus \mathbb{L}_{(0,\epsilon I)} = \mathbb{L}_{(0,D)} & \text{if} \quad t_\mathsf{k} \in \mathbb{T}_e,\ \epsilon \downarrow 0. \end{cases}$$

A suitable value for ς minimizes the trace of $(1+\varsigma^{-1})D + (1+\varsigma)H_\mathsf{e}(t_\mathsf{k})$.

Now, combining the measurement information in (13.22) with the above noise term $\tilde{v}_d$ and the process model in (13.1) results in a new (implied) measurement $z(t_\mathsf{k})$ having the following measurement model and measurement realizations, for a received $y(t_\mathsf{e})$ and a computed $\hat{y}_\mathsf{e}(t_\mathsf{k})$:

$$\text{model} \quad z(t_\mathsf{k}) = Cx(t_\mathsf{k}) + v_s(t_\mathsf{k}) + \tilde{v}_d(t_\mathsf{k}), \quad (13.23)$$

$$\text{realization} \quad z(t_\mathsf{k}) = \begin{cases} \hat{y}_\mathsf{e}(t_\mathsf{k}) & \text{if} \quad t_\mathsf{k} \in \mathbb{T}_p \setminus \mathbb{T}_e, \\ y(t_\mathsf{e}) & \text{if} \quad t_\mathsf{k} \in \mathbb{T}_e. \end{cases} \quad (13.24)$$

The stochastic measurement noise still follows $v_s(t_\mathsf{k}) \sim \mathcal{G}(0,V)$, while the deterministic measurement noise $\tilde{v}_d = v_d + e$ follows $\tilde{v}_d(t_\mathsf{k}) \in \mathbb{L}_{(0,E(t_\mathsf{k}))}$ and

$$E(t_\mathsf{k}) := \begin{cases} (1+\varsigma^{-1})D + (1+\varsigma)H_\mathsf{e}(t_\mathsf{k}) & \text{if} \quad t_\mathsf{k} \in \mathbb{T}_p \setminus \mathbb{T}_e, \\ D & \text{if} \quad t_\mathsf{k} \in \mathbb{T}_e. \end{cases}$$

EXAMPLE 13.2: Ellipsoidal sets for event sampling strategies One can derive that the event sampling strategies send-on-delta and matched sampling, as presented in Section 13.4.1, will result in an ellipsoidal shaped triggering set $\mathbb{H}(\mathsf{e},t_\mathsf{k})$. The center and shape matrix of this set directly define values for $\hat{y}_\mathsf{e}(t_\mathsf{k})$ and $H_\mathsf{e}(t_\mathsf{k})$ in (13.21), yielding

- Send-on-delta: $\hat{y}_\mathsf{e}(t_\mathsf{k}) = y(t_{\mathsf{e}-1})$ and $H_\mathsf{e}(t_\mathsf{k}) = \Delta I$.
- Matched sampling: In case the sensor employs the asynchronous Kalman filter of Remark 13.2 for computing the divergence, with $\mathrm{cov}(w_s) = W$ and $\mathrm{cov}(v_s) = V$, then $\hat{y}_\mathsf{e}(t_\mathsf{k}) = Cx_2(t_\mathsf{k}^-)$ and $H_\mathsf{e}(t_\mathsf{k}) = 2(\Delta - \alpha)^{-1}(V^{-1}CP_1(t_\mathsf{k})P_2^{-1}(t_\mathsf{k})P_1(t_\mathsf{k})CV^{-1})^{-1}$, where $\alpha = 0.5\left(\log|P_2(t_\mathsf{k})||P_2(t_\mathsf{k})|^{-1} + \mathrm{tr}(P_2^{-1}(t_\mathsf{k})P_1(t_\mathsf{k})) - n\right)$.
- Some illustrative examples of the ellipsoidal sets for send-on-delta and matched sampling are found in Figure 13.5.

13.6.2 Estimation Formulas

The *h*EBSE exploits the (implied) measurement values of $z(t_\mathsf{k})$ as proposed in (13.23), for all $t_\mathsf{k} \in \mathbb{T}$. The *h*EBSE aims to solve the estimation problem for the state representation $x(t_\mathsf{k}) = \hat{x}(t_\mathsf{k}) + \tilde{x}_d(t_\mathsf{k}) + \tilde{x}_s(t_\mathsf{k})$. The underlying idea is to compute a state estimate $\hat{x}$ that minimizes the (maximum possible) mean squared error (MSE) of $\hat{x} - x$ in the presence of both stochastic and deterministic noises (or uncertainties). For clarity, let us point out that the error associated with the state estimate $\hat{x}(t)$ is composed of a stochastic and a deterministic part, that is,

$$\hat{x}(t_\mathsf{k}) - x(t_\mathsf{k}) = \tilde{x}_s(t_\mathsf{k}) + \tilde{x}_d(t_\mathsf{k}),$$

where

$$\tilde{x}_s(t_\mathsf{k}) \sim \mathcal{G}\big(0, P(t_\mathsf{k})\big) \quad \text{and} \quad \tilde{x}_d(t_\mathsf{k}) \in \mathbb{L}_{0,X(t_\mathsf{k})}.$$

The advantage of assuming an ellipsoidal set-inclusion for $\tilde{x}_d$ and a Gaussian distribution for $\tilde{x}_s$ is that estimation errors are characterized by $P \succ 0$ and $X \succ 0$. Since the deterministic error is nonstochastic and independent from stochastic errors, note that the considered MSE then yields

$$\begin{aligned} &\mathbb{E}\big[\big(\hat{x}(t_\mathsf{k}) - x(t_\mathsf{k})\big)^\top\big(\hat{x}(t_\mathsf{k}) - x(t_\mathsf{k})\big)\big] \\ &\quad = \underbrace{\mathbb{E}\big[\tilde{x}_s^\top(t_\mathsf{k})\tilde{x}_s(t_\mathsf{k})\big]}_{=\mathrm{tr}\left(P(t_\mathsf{k})\right)} + \underbrace{\tilde{x}_d^\top(t_\mathsf{k})\tilde{x}_d(t_\mathsf{k})}_{\leq \mathrm{tr}\left(X(t_\mathsf{k})\right)} \\ &\quad \leq \mathrm{tr}\big(P(t_\mathsf{k}) + X(t_\mathsf{k})\big)\,. \end{aligned} \quad (13.25)$$

Thus, the MSE is bounded by the trace of $P(t_k) + X(t_k)$. The estimator proposed in [26] forms the basis of the *h*EBSE, as it minimizes exactly this bound. Additional to standard Kalman filtering, the estimate $\hat{x}$ is associated not only with an error-covariance P but also with a error-shape matrix X. The values of these matrices and of the state estimate $\hat{x}$ are computed in line with standard estimation approaches, that is, with a prediction step and a measurement update.

Step 1 Compute the predicted values* $\hat{x}(t_k^-)$, $P(t_k^-)$ and $X(t_k^-)$ given their prior results at $k-1$. Note that the process model in (13.1) is linear and that $w_s(t_k)$ is unbiased and characterized by $W \succ 0$. Moreover, the estimation error of $\hat{x}(t_k)$ is characterized by positive definite matrices $P(t_k^-)$ and $X(t_k^-)$ as well. These prerequisites are in line with standard Kalman filtering (extended with shape matrices) and it was shown in [26] that a similar prediction step can be employed here as well, that is,

$$\begin{aligned} \hat{x}(t_k^-) &= A_{\tau_k}\hat{x}(t_{k-1}), \\ P(t_k^-) &= A_{\tau_k}P(t_{k-1})A_{\tau_k}^\top + B_{\tau_k}WB_{\tau_k}^\top, \\ X(t_k^-) &= A_{\tau_k}X(t_{k-1})A_{\tau_k}^\top. \end{aligned} \tag{13.26}$$

Recall that $\tau_k := t_k - t_{k-1}$ is the sampling time. Evidently, this prediction can be computed in closed form and only differs from a Kalman filter by the additional third expression determining $X(t_k^-)$.

Step 2 Compute the updated values $\hat{x}(t_k)$, $P(t_k)$, and $X(t_k)$, given their prediction results from Step 1 and the measurement $z(t_k)$ of (13.23). Again, the process model in (13.1) is linear and the unbiased measurement noises $\tilde{v}_d(t_k)$ and $v_s(t_k)$ are characterized by $E(t_k) \succeq 0$ and $V \succ 0$, respectively, where $\tilde{v}_d$ is a substitute of v_d to include the event triggering set. As such, one can employ an unbiased update expression in line with any linear estimator, for some gain $K(t_k) \in \mathbb{R}^{n\times m}$, that is,

$$\hat{x}(t_k) = (I - K(t_k)C)\hat{x}(t_k^-) + K(t_k)z(t_k). \tag{13.27}$$

In line with the above expression, the updated error-covariance and error-shape matrices also follow standard Kalman filtering expressions, yielding

$$\begin{aligned} P(t_k) &= \big(I - K(t_k)C\big)P(t_k^-)\big(I - K(t_k)C\big)^\top \\ &\quad + K(t_k)VK(t_k)^\top, \end{aligned} \tag{13.28}$$

$$\begin{aligned} X(t_k) &= \tfrac{1}{1-\omega(t_k)}\big(I - K(t_k)C\big)X(t_k^-)\big(I - K(t_k)C\big)^\top \\ &\quad + \tfrac{1}{\omega(t_k)}K(t_k)E(t_k)K(t_k)^\top. \end{aligned} \tag{13.29}$$

*The notation t_k^- is used to emphasize the predictive character of a variable at t_k.

The parameter $\omega(t_k) \in (0,1)$ in (13.29) guarantees that the shape matrix $X(t_k)$ corresponds to an outer ellipsoidal approximation of two ellipsoidal sets: the sets being a weighted prediction error and a measurement error, that is, $\mathbb{L}_{\left(0,(I-K(t_k)C)\,X(t_k^-)\,(I-K(t_k)C)\right)}$ and $\mathbb{L}_{\left(0,K(t_k)\,E(t_k)\,K(t_k)^\top\right)}$.

Results in [26] point out that the gain $K(t_k)$ is given by

$$\begin{aligned} K(t_k) = &\Big(P(t_k^-)\,C^\top + \tfrac{1}{1-\omega(t_k)}X(t_k^-)\,C^\top\Big) \\ &\cdot \Big(C\,P(t_k^-)\,C^\top + \tfrac{1}{1-\omega(t_k)}C\,X(t_k^-)\,C^\top \\ &\quad + V + \tfrac{1}{\omega}E(t_k)\Big)^{-1}. \end{aligned} \tag{13.30}$$

A one-dimensional convex optimization problem for $\omega^{\mathrm{opt}} \in (0,1)$ that minimizes the posterior MSE bound in (13.25) remains to be solved, for example, with the aid of Brent's method.

REMARK 13.4 The derived gain (13.30) embodies a systematic and consistent generalization of the standard Kalman filter for additional unknown but bounded uncertainties. Accordingly, K in (13.30) reduces to the standard Kalman gain in the absence of set-membership errors, that is, $Q = 0$, $E(t_k) = 0$ implying that $X(t_k) = 0$ for all $t_k \in \mathbb{T}$. In the opposite case of vanishing error covariance matrices, the *h*EBSE yields a deterministic estimator of intersecting ellipsoidal sets.

REMARK 13.5 The sum of the error matrices is expressed via

$$\begin{aligned} P(t_k) + X(t_k) = &\Big(\omega(t_k)\big(\omega(t_k)P(t_k^-) + X(t_k^-)\big)^{-1} \\ &+ (1-\omega(t_k))C^\top \\ &\times \big((1-\omega(t_k))V + E(t_k)\big)^{-1}C\Big)^{-1}, \end{aligned} \tag{13.31}$$

which can be utilized to determine ω^{opt} that minimizes the right-hand side bound in (13.25). The special cases $\omega^{\mathrm{opt}} = 0$ or $\omega^{\mathrm{opt}} = 1$ will not be considered.

This completes the hybrid EBSE resulting in a correct description of the estimation results for including the event triggering set $\mathbb{H}(\mathsf{e}, t_k)$ into the estimation results. Before continuing with an observation case study, let us first point out the stability of estimation errors.

13.6.3 Asymptotic Analysis

The hybrid EBSE is said to be stable iff both $P(t_k)$ and $X(t_k)$ have finite eigenvalues for $t_k \to \infty$. Proving

stability is done in two steps:

1. Introduce a $\Gamma(t_k)$, such that $P(t_k) + X(t_k) \preceq \Gamma(t_k)$ holds for all $t_k \in \mathbb{T}$.
2. Show that $\Gamma(t_k) \preceq \Sigma(t_k)$, for some $\Sigma(t_k)$ being the result of a standard, periodic Kalman filter.

Then, the proposed estimator enjoys the same stability conditions as a (standard) periodic Kalman filter would have, that is, depending on detectability and observability properties. For clarity of the presented results, it is assumed that the scalar weight ω will be constant at all sampling instants, that is, the hybrid EBSE employs $\omega(t_k) = \omega$ in (13.28), (13.29), (13.30), and (13.31) for all $t_k \in \mathbb{T}$, though the results can be generalized to weights varying in time.

Let us start with the first step where $P(t_k) + X(t_k) \preceq \Gamma(t_k)$. After this step, one can guarantee that iff $\Gamma(t_k) \succ 0$ is asymptotically stable, then both $P(t_k)$ and $X(t_k)$ shall be asymptotically stable as well. In line with the results of (13.26) and of (13.31), let us introduce the following update equation for $\Gamma(t_k)$, that is,

$$\begin{aligned}\Gamma(t_k^-) &= A_{\tau_k}\Gamma(t_{k-1})A_{\tau_k}^\top + B_{\tau_k}WB_{\tau_k}^\top,\\ \Gamma(t_k)&\\ &= \big(\omega\big(\Gamma(t_k^-)\big)^{-1} + (1-\omega)C^\top\big((1-\omega)V + E(t_k)\big)^{-1}C\big)^{-1}.\end{aligned} \tag{13.32}$$

Theorem 13.3

Consider $P(t_k)$ and $X(t_k)$ of the hybrid EBSE, for some constant $\omega \in (0,1)$, and consider $\Gamma(t_k)$ in (13.32). Further, let $\Gamma(0) := P(0) + X(0)$. Then, $P(t_k) + X(t_k) \prec \Gamma(t_k)$ holds for all $t_k \in \mathbb{T}$.

The proof of this theorem is found in the appendix.

Let us continue with the second step of this asymptotic analysis, for which we will introduce $\Sigma(t_n)$ computed via an update equation similar to a time-periodic Kalman filter, that is, for all time-periodic instants $t_n \in \mathbb{T}_p$,

$$\begin{aligned}\Sigma(t_n^-) &= \bar{A}\Sigma(t_{n-1})\bar{A}^\top + \bar{B}W\bar{B}^\top,\\ \Sigma(t) &= \big(\omega^{-\kappa+1}\big(\Sigma(t^-)\big)^{-1}\\ &\quad + (1-\omega)C^\top\big((1-\omega)V + E(t_n)\big)^{-1}C\big)^{-1}.\end{aligned} \tag{13.33}$$

The scalar $\kappa \in (0,1)$ is an upper bound on the amount of events that can occur between two consecutive periodic sample instants (t_n) and (t_{n-1}). The constant system matrices above are defined as $\bar{A} := A_{\tau_s}$ and $\bar{B} := B_{\tau_s}$.

Theorem 13.4

Consider $\Gamma(t_k)$ in (13.32) and $\Sigma(t_n)$ in (13.33) and let $\Sigma(0) := \Gamma(0)$. Then, $\Gamma(t_k) \prec \Sigma(t_n)$ holds for all $t_k = t_n$ and $t_n \in \mathbb{T}_p$.

The proof of this theorem is found in the appendix. Moreover, the results in Theorem 13.4 guarantee that the hybrid EBSE proposed has asymptotically stable estimation results in case $(\bar{A}, C)$ is detectable.

13.7 Illustrative Case Study

Results of the stochastic and hybrid event-based state estimator are studied here in terms of estimation errors for tracking a 1D object. The process model in line with (13.1) is a double integrator, that is,

$$\begin{aligned}x(t) &= \begin{bmatrix}1 & \tau\\ 0 & 1\end{bmatrix}x(t-\tau) + \begin{bmatrix}\frac{1}{2}\tau^2\\ \tau\end{bmatrix}a(t-\tau)\,,\\ y(t) &= \begin{bmatrix}1 & 0\end{bmatrix}x(t) + v_s(t)\,.\end{aligned}$$

The state vector $x(t)$ combines the object's position and speed. Further, $a(t) = \frac{1}{30}t \cdot \cos(\frac{1}{10}t)$ denotes the object's acceleration, while only the position is measured in $y(t)$. Since acceleration is assumed unknown, the process model in (13.1) is characterized with a process noise $w(t) := a(t)$. During the simulation, the acceleration is bounded by $|a(t)| \leq 0.9$, due to which a suitable covariance in line with [6] is $\mathrm{cov}(a(t)) = 1.1$, resulting in an unbiased distribution $p(w(t))$ with covariance $W = 1.1$. Further, the sampling time is $\tau_s = 0.1$ seconds and the sensor noise covariance is set to $V = 2 \cdot 10^{-3}$. The object's true position, speed, and acceleration are depicted in Figure 13.6.

The *h*EBSE of Section 13.6 combining stochastic and set-membership measurement information is compared to the *s*EBSE presented in 13.5.1 limited to stochastic representations. Both estimators start with the initial estimation results $\hat{x}(0) = \begin{pmatrix}0.1 & 0.1\end{pmatrix}^\top$ and $P(0) = 0.01 \cdot I$,

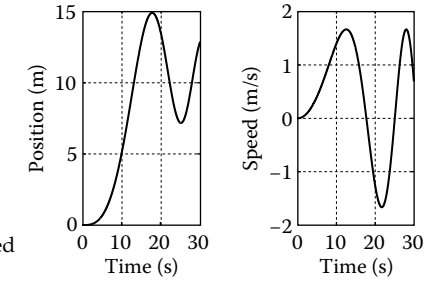

FIGURE 13.6
The position, speed, and acceleration of the tracked object.

while $X(0) = 0$ is chosen as the initial ellipsoidal shape matrix for the *h*EBSE. Next, the measurement information of both EBSEs is characterized.

hEBSE

Measurement information of the *h*EBSE is represented by the implied measurement $z(t) = Cx(t) + v_s(t) + \tilde{v}_d(t)$. Note that the original measurement is only affected by stochastic noise and that $v_d(t) \in \emptyset$, due to which $\tilde{v}_d(t) = e(t)$ is characterized by an ellipsoidal approximation $e(t) \in \mathbb{L}_{0,E}$ of the event triggering set. In case of an event instant $t \in \mathbb{T}_e$, the measurement $y(t_\mathsf{e})$ is received and one obtains that $z(t) = y(t_\mathsf{e})$, that is, $e(t_\mathsf{e}) \in \emptyset$ and $E(t) = 0$. At periodic time instants $t \in \mathbb{T}_p$, one has the information that $y(t) \in \mathbb{H}(\mathsf{e}, t)$. This ellipsoidal set $\mathbb{H}(\mathsf{e}, t)$ can be characterized with a "mass"-center, yielding an estimate of $y(t)$ and an ellipsoidal error-set resulting in an characterization of $e(t) \in \mathbb{L}_{0,E(t)}$ via $E(t) = H_\mathsf{e}(t)$. Suitable realizations of $z(t)$ and $E(t)$ for the two employed event strategies were already given in Example 13.2, where $\Phi(t) := 2(\Delta - \alpha)^{-1}(V^{-1}CP_1(t)P_2^{-1}(t)P_1(t)CV^{-1})^{-1}$, that is,

Send-on-delta:

$$z(t) = y(t_\mathsf{e}), \qquad E(t) = 0, \qquad \forall t \in \mathbb{T}_e,$$
$$z(t) = y(t_{\mathsf{e}-1}), \qquad E(t) = \Delta^2, \qquad \forall t \in \mathbb{T}_p,$$

Matched sampling:

$$z(t) = y(t_\mathsf{e}), \qquad E(t) = 0, \qquad \forall t \in \mathbb{T}_e,$$
$$z(t) = CA_{t-t_{\mathsf{e}-1}}\hat{x}(t_{\mathsf{e}-1}), \qquad E(t) = \Phi(t), \qquad \forall t \in \mathbb{T}_p.$$

sEBSE

Measurement information of the *s*EBSE is represented by a single Gaussian PDF, that is, $p(y(t)) = \mathcal{G}\big(y(t), \hat{y}(t), R(t)\big)$ for some (estimated) measurement value $\hat{y}(t)$ and covariance matrix $R(t) = V(t) + U(t)$. Herein, $V(t)$ is the covariance of the stochastic measurement noise $v_s(t)$, while $U(t)$ is a covariance due to any implied measurement information as it is treated as an additional stochastic noise. In case of an event instant $t \in \mathbb{T}_e$ the measurement $y(t_\mathsf{e})$ is received and one obtains that $\hat{y}(t) = y(t_\mathsf{e})$ and $U(t) = 0$. At periodic time instants $t \in \mathbb{T}_p$, one has the information that $y(t) \in \mathbb{H}(\mathsf{e}, t)$, which is then turned into a particular value for $\hat{y}(t)$ and $U(t)$. A suitable characterization of $\hat{y}(t)$ and $U(t)$ for the two employed event sampling strategies were already given in Example 13.2, where $\Phi(t) := 2(\Delta - \alpha)^{-1}(V^{-1}CP_1(t)P_2^{-1}(t)P_1(t)CV^{-1})^{-1}$, that is,

Send-on-delta:

$$\hat{y}(t) = y(t_\mathsf{e}), \qquad U(t) = 0, \qquad \forall t \in \mathbb{T}_e,$$
$$\hat{y}(t) = y(t_{\mathsf{e}-1}), \qquad U(t) = \frac{3}{4}\Delta^2, \qquad \forall t \in \mathbb{T}_p,$$

Matched sampling:

$$\hat{y}(t) = y(t_\mathsf{e}), \qquad U(t) = 0, \qquad \forall t \in \mathbb{T}_e,$$
$$\hat{y}(t) = CA_{t-t_{\mathsf{e}-1}}\hat{x}(t_{\mathsf{e}-1}), \qquad U(t) = \frac{1}{4}\Phi(t), \qquad \forall t \in \mathbb{T}_p.$$

Figure 13.7 until Figure 13.10 depict the actual squared estimation error, that is, $\|\hat{x}(t) - x(t)\|_2^2$, in comparison to the modeled estimation error, that is, $\mathrm{tr}(P(t))$ for the *s*EBSE and $\mathrm{tr}(P(t)) + \mathrm{tr}(X(t))$ for the *h*EBSE. The results depicted were obtained after averaging the outcome of 1000 runs of the considered simulation case study.

Figures 13.7 and 13.8 depict the estimation results of the *h*EBSE and the *s*EBSE, respectively, when matched sampling is employed as the event sampling strategy. Although it is not pointed out in the figures, it is worth mentioning that the *h*EBSE triggered a total amount

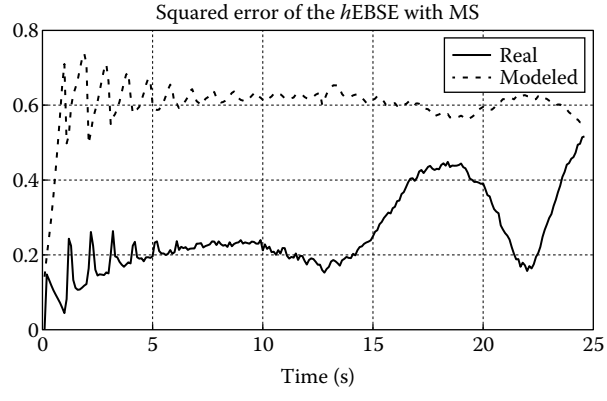

FIGURE 13.7

Simulation results for *matched sampling* (MS) in combination with the *h*EBSE allowing stochastic and set-membership representations. The real squared estimation error $\|\hat{x}(t) - x(t)\|_2^2$ is depicted versus the modeled (bound) of the estimation error $\mathrm{tr}(P(t)) + \mathrm{tr}(X(t))$.

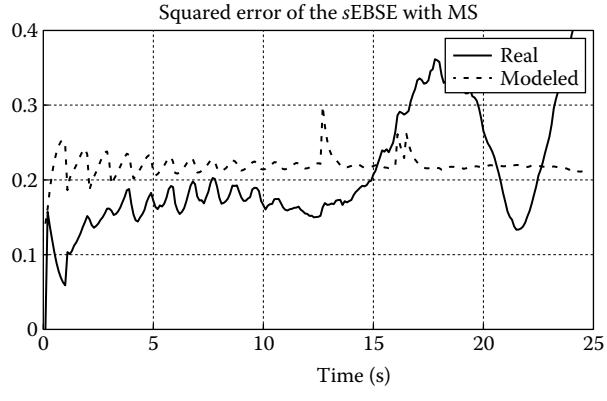

FIGURE 13.8

Simulation results for *matched sampling* (MS) in combination with the *s*EBSE limited to stochastic representations. The real squared estimation error $\|\hat{x}(t) - x(t)\|_2^2$ is depicted versus the modeled (bound) of the estimation error $\mathrm{tr}(P(t))$.

of 31 events (on average), while the *s*EBSE triggered 40 events (on average). Further, the real squared estimation error of both EBSEs considered is comparable. Hence, the *h*EBSE has similar estimation results with fewer events triggered, due to which less measurement samples are required saving communication resources. Yet, the main advantage of the *h*EBSE is the modeled bound on the estimation error. Figure 13.7 indicates that this modeled bound is conservative when the *h*EBSE is employed, which is not the case for the *s*EBSE depicted in Figure 13.8. This means that the *h*EBSE gives a better guarantee that the real estimation error stays within the bound as it is computed by the estimator. Such a property is important when estimation results are used for control purposes.

Figures 13.9 and 13.10 depict the estimation results of the *h*EBSE and the *s*EBSE, respectively, when send-on-delta is employed as the event sampling strategy. Since this event sampling strategy does not depend on previous estimation results but merely on the previous measurement sample, both estimators received the events at the same time instants giving a total of 115 events. Note that this is an increase of events by a factor of 3 to 4 when compared to the EBSEs in combination with matched sampling. Yet, this increase of events and thus of measurement samples is not reflected in a corresponding

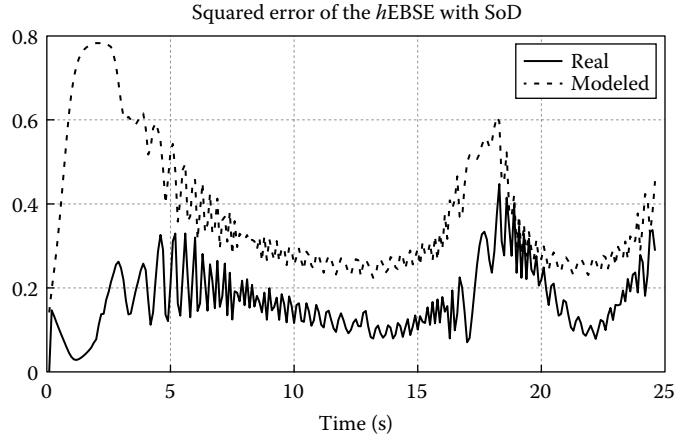

FIGURE 13.9

Simulation results for *send-on-delta* (SoD) in combination with the *h*EBSE allowing stochastic and set-membership representations. The real squared estimation error $\|\hat{x}(t) - x(t)\|_2^2$ is depicted versus the modeled (bound) of the estimation error $\mathrm{tr}(P(t)) + \mathrm{tr}(X(t))$.

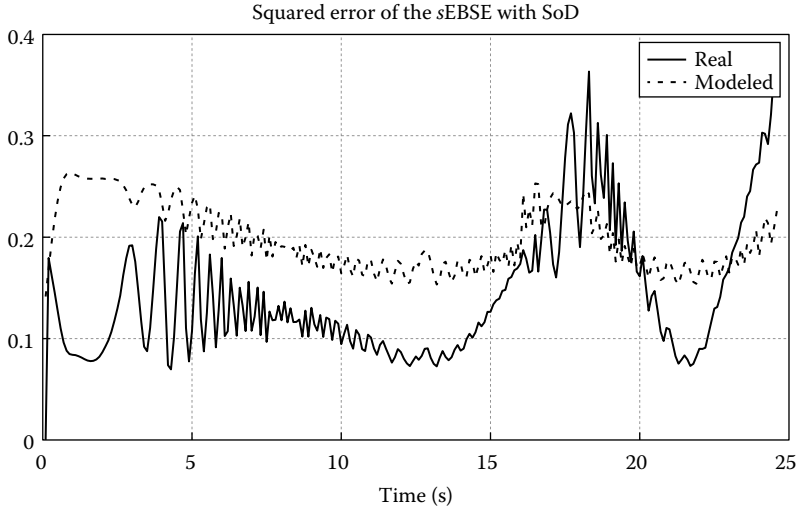

FIGURE 13.10

Simulation results for *send-on-delta* (SoD) in combination with the *s*EBSE limited to stochastic representations. The real squared estimation error $\|\hat{x}(t) - x(t)\|_2^2$ is depicted versus the modeled (bound) of the estimation error $\mathrm{tr}(P(t))$.

decrease of estimation errors. Further, similar conclusions can be drawn from the estimation results with send-on-delta when comparing Figures 13.9 and 13.10. Again, the squared estimation error of the two considered EBSEs is comparable and the main advantage of the *h*EBSE is in the improved bound of the modeled estimation error.

Therefore, a fair conclusion of the *h*EBSE is that similar estimation errors are achieved when compared to *s*EBSE, although the *modeled* estimation error of the *h*EBSE is a far better bound on *real* estimation errors. Similar results are expected when comparing the *h*EBSE with the deterministic *d*EBSE, as in the latter EBSE noises should be represented as a set-membership. As such, the *h*EBSE is advantageous in networked control systems where estimation results are being used by a (stabilizing) controller.

13.8 Conclusions

In networked systems, high measurement frequencies may rapidly exhaust communication bandwidth and power resources when sensor data must be transmitted periodically to the state estimator. The transmission rate can significantly be reduced if an event-based strategy is employed for sampling sensor data. "send-on-delta" and "matched sampling" have been discussed as examples of such strategies. This chapter discussed several ideas to process these event sampled measurements. Typical estimation approaches perform a measurement update whenever an event is triggered, that is, at the event instants when a new measurement is received. However, observation and automation systems are mainly designed to rely on time-periodic estimation results. The time gap between events and periodic instants can simply be bridged by prediction steps, but additional knowledge then remains untapped: as long as no event is triggered, the actual sensor value does not fulfill the event-sampling criterion, thereby implying that it did not cross the edge of a particular closed set. Recent estimators do exploit this implied measurement information and three of them were discussed, here; one restricted to stochastic noise representations, one restricted to set membership noise representations, and one hybrid solution allowing both stochastic and set membership representations. The latter one is more advantageous, as measurement and process noise are typically characterized as a stochastic random vector, while the implied information results in a set membership property on the sensor value. Prospective research focuses also on unreliable networks, where delays and packet losses have to be taken into account.

Appendix A Proof of Theorem 13.3

Let us introduce $R(t_k) := (1-\omega)C^\top\big((1-\omega)V + E(t_k)\big)^{-1}C$. Then, the update formulas of $\Gamma(t_k)$ in (13.32), yields

$$\begin{aligned}\Gamma(t_k^-) &= A_{\tau_k}\Gamma(t_{k-1})A_{\tau_k}^\top + B_{\tau_k}WB_{\tau_k}^\top,\\ \Gamma(t) &= \Big(\omega\big(\Gamma(t_k^-)\big)^{-1} + R(t_k)\Big)^{-1}, \quad \forall t_k \in \mathbb{T}.\end{aligned} \tag{13.34}$$

Similarly, let us derive the update equation for $P(t) + X(t)$ in line with the results in (13.26) and (13.31), that is,

$$\begin{aligned}&P(t_k^-) + X(t_k^-)\\ &\quad = A_{\tau_k}\left(P(t_{k-1}) + X(t_{k-1})\right)A_{\tau_k}^\top + B_{\tau_k}WB_{\tau_k}^\top,\\ &P(t_k) + X(t_k)\\ &\quad = \Big(\omega\big(\omega P(t_k^-) + X(t_k^-)\big)^{-1} + R(t_k)\Big)^{-1}, \quad \forall t_k \in \mathbb{T}.\end{aligned} \tag{13.35}$$

The inequality $P(t_k) + X(t_k) \prec \Gamma(t_k)$, for all $T_k \in \mathbb{T}$, is proven by induction: first show that $P(t_1) + X(t_1) \prec \Gamma(t_1)$ when $\Gamma(0) = P(0) + X(0)$, followed by a proof of $P(t_k) + X(t_k) \prec \Gamma(t_k)$ iff $P(t_{k-1}) + X(t_{k-1}) \prec \Gamma(t_{k-1})$.

The first step of induction starts from $\Gamma(0) = P(0) + X(0)$. The prediction $\Gamma(t_1^-)$ in (13.34) and $P(t_1^-) + X(t_1^-)$ in (13.35) give that $\Gamma(t_1^-) = P(t_1^-) + X(t_1^-)$. Substituting this result in the update equation of $\Gamma(t_1)$ in (13.34) yields

$$\Gamma(t_1) = \Big(\omega\big(P(t_1^-) + X(t_1^-)\big)^{-1} + R(t_1)\Big)^{-1}.$$

Since $\omega \in (0,1)$, this latter equality further implies that

$$\begin{aligned}\Gamma(t_1) &\succ \Big(\omega\big(\omega P(t_1^-) + X(t_1^-)\big)^{-1} + R(t_1)\Big)^{-1}, &(13.36)\\ &= P(t_1) + X(t_1), &(13.37)\end{aligned}$$

which proves the first step of induction.

The second step starts from $P(t_{k-1}) + X(t_{k-1}) \prec \Gamma(t_{k-1})$. The prediction $\Gamma(t_k^-)$ in (13.34) and $P(t_k^-) + X(t_k^-)$ in (13.35) give that $P(t_k^-) + X(t_k^-) \prec \Gamma(t_k^-)$. Substituting this result in the update equation of $\Gamma(t_k)$ in (13.34) yields

$$\Gamma(t_k) \succ \Big(\omega\big(P(t_k^-) + X(t_k^-)\big)^{-1} + R(t_k)\Big)^{-1}.$$

Since $\omega \in (0,1)$, this latter equality further implies that

$$\begin{aligned}\Gamma(t_k) &\succ \Big(\omega\big(\omega P(t_k^-) + X(t_k^-)\big)^{-1} + R(t_k)\Big)^{-1}, &(13.38)\\ &= P(t_k) + X(t_k), &(13.39)\end{aligned}$$

which proves the second step of induction and thereby Theorem 13.3.

Appendix B Proof of Theorem 13.4

Let us introduce $R(t) := (1-\omega)C^\top\big((1-\omega)V + E(t)\big)^{-1}C$. Then, the update formulas of $\Gamma(t_\mathsf{k})$ in (13.32), yields

$$\begin{aligned}\Gamma(t_\mathsf{k}^-) &= A_{\tau_\mathsf{k}}\Gamma(t_{\mathsf{k}-1})A_{\tau_\mathsf{k}}^\top + B_{\tau_\mathsf{k}}WB_{\tau_\mathsf{k}}^\top,\\ \Gamma(t_\mathsf{k}) &= \Big(\omega\big(\Gamma(t_\mathsf{k}^-)\big)^{-1} + R(t_\mathsf{k})\Big)^{-1}, \quad \forall t_\mathsf{k}\in\mathbb{T}.\end{aligned} \tag{13.40}$$

Similarly, the update formulas of $\Sigma(t_\mathsf{n})$ in (13.33) are as follows:

$$\begin{aligned}\Sigma(t_\mathsf{n}^-) &= \bar{A}\left(\Sigma(t_{\mathsf{n}-1})\right)\bar{A}^\top + \bar{B}W\bar{B}^\top,\\ \Sigma(t_\mathsf{n}) &= \Big(\omega^{-\kappa+1}\big(\Sigma(t_\mathsf{n}^-)\big)^{-1} + R(t_\mathsf{n})\Big)^{-1}, \quad \forall t_\mathsf{n}\in\mathbb{T}_p.\end{aligned} \tag{13.41}$$

The following result is instrumental for proving Theorem 13.4. To that extent, let $\kappa\in\mathbb{Z}_+$ be the amount of event instants in between the two consecutive time-periodic instants $\underline{t}-\tau_s$ and $\underline{t}$, or differently, $\underline{t}-\tau_s = t_{\mathsf{k}-\kappa-1} < t_{\mathsf{k}-\kappa} < t_{\mathsf{k}-\kappa+1} < \ldots < t_{\mathsf{k}-1} < t_\mathsf{k} = \underline{t}$. Further, let us introduce the time instant $\underline{t}\in\mathbb{T}_p$, such that $t_\mathsf{k} = \underline{t}$ and $t_\mathsf{n} = \underline{t}$ for some $\mathsf{k},\mathsf{n}\in\mathbb{Z}_+$. As $\tau_s\in\mathbb{R}_+$ is the sampling time, one has that $t_{\mathsf{n}-1} = \underline{t}-\tau_s$ and $t_{\mathsf{k}-\kappa-1} = \underline{t}-\tau_s$, that is, $t_{\mathsf{n}-1} = t_{\mathsf{k}-\kappa-1}$.

Lemma 13.1

Let us consider $\Gamma(\underline{t})$ characterized by (13.40) and $\Sigma(t)$ by (13.41), for some $\underline{t}\in\mathbb{T}_p$, while satisfying $\Gamma(\underline{t}-\tau_s)\preceq\Sigma(\underline{t}-\tau_s)$. Then, $\Gamma(\underline{t}^-)\preceq\omega^{-\kappa}\Sigma(\underline{t}^-)$ holds for any suitable k,n such that $\underline{t} = t_\mathsf{k}$ and $\underline{t} = t_\mathsf{n}$.

PROOF The proof of this lemma start with the inequality that

$$\Gamma(t_\mathsf{k})\preceq\omega^{-1}\Gamma(t_\mathsf{k}^-), \quad \forall t_\mathsf{k}\in\mathbb{T}, \quad \text{see (13.40).} \tag{13.42}$$

When substituting this result in the prediction step of (13.40), one can further derive that

$$\begin{aligned}\Gamma(t_\mathsf{k}^-) &= \Big(A_{\tau_{\mathsf{k}-1}}\Gamma(t_{\mathsf{k}-1})A_{\tau_{\mathsf{k}-1}}^\top + B_{\tau_{\mathsf{k}-1}}WB_{\tau_{\mathsf{k}-1}}^\top\Big),\\ &\preceq \omega^{-1}\Big(A_{\tau_{\mathsf{k}-1}}\Gamma(t_{\mathsf{k}-1}^-)A_{\tau_{\mathsf{k}-1}}^\top + B_{\tau_{\mathsf{k}-1}}WB_{\tau_{\mathsf{k}-1}}^\top\Big),\\ &\preceq \omega^{-2}\Big(A_{\tau_{\mathsf{k}-1}}A_{\tau_{\mathsf{k}-2}}\Gamma(t_{\mathsf{k}-2}^-)A_{\tau_{\mathsf{k}-2}}^\top A_{\tau_{\mathsf{k}-1}}^\top\\ &\qquad + A_{\tau_{\mathsf{k}-1}}B_{\tau_{\mathsf{k}-2}}WB_{\tau_{\mathsf{k}-2}}^\top A_{\tau_{\mathsf{k}-1}}^\top + B_{\tau_{\mathsf{k}-1}}WB_{\tau_{\mathsf{k}-1}}^\top\Big).\end{aligned}$$

From the definition of A_τ and B_τ in Section 13.3, one obtains that $A_{\tau_i+\tau_{i-1}} = A_{\tau_i}A_{\tau_{i-1}}$ and $B_{\tau_i+\tau_{i-1}} = A_{\tau_i}B_{\tau_{i-1}} + B_{\tau_i}$ for any bounded $\tau_i > 0$ and $\tau_{i-1} > 0$. Substituting this result in the above inequality of $\Gamma(t_\mathsf{k}^-)$ thus results in

$$\begin{aligned}\Gamma(t_\mathsf{k}^-) &\preceq \omega^{-2}\Big(A_{\tau_{\mathsf{k}-1}+\tau_{\mathsf{k}-2}}\Gamma(t_{\mathsf{k}-2}^-)A_{\tau_{\mathsf{k}-1}+\tau_{\mathsf{k}-2}}^\top\\ &\qquad + B_{\tau_{\mathsf{k}-1}+\tau_{\mathsf{k}-2}}WB_{\tau_{\mathsf{k}-1}+\tau_{\mathsf{k}-2}}^\top\Big),\\ &\preceq \omega^{-\kappa}\Big(A_{\sum_{i=1}^\kappa\tau_{\mathsf{k}-i}}\Gamma(t_{\mathsf{k}-\kappa}^-)A_{\sum_{i=1}^\kappa\tau_{\mathsf{k}-i}}^\top\\ &\qquad + B_{\sum_{i=1}^\kappa\tau_{\mathsf{k}-i}}WB_{\sum_{i=1}^\kappa\tau_{\mathsf{k}-i}}^\top\Big).\end{aligned}$$

Note that $\Gamma(t_{\mathsf{k}-\kappa}^-) = A_{\tau_{\mathsf{k}-\kappa-1}}\Gamma(t_{\mathsf{k}-\kappa-1})A_{\tau_{\mathsf{k}-\kappa-1}}^\top + B_{\tau_{\mathsf{k}-\kappa-1}}WB_{\tau_{\mathsf{k}-\kappa-1}}^\top$, which after substituting in the above inequality gives that

$$\Gamma(t_\mathsf{k}^-)\preceq\omega^{-\kappa}\left(A_{\delta_{\mathsf{k},\kappa-1}}\Gamma(t_{\mathsf{k}-\kappa-1})A_{\delta_{\mathsf{k},\kappa-1}}^\top + B_{\delta_{\mathsf{k},\kappa-1}}WB_{\delta_{\mathsf{k},\kappa-1}}^\top\right) \tag{13.43}$$

where $\delta_{\mathsf{k},\kappa-1} := \sum_{i=1}^{\kappa+1}\tau_{\mathsf{k}-i}$. The lemma considers time-periodic instants, that is, $t_\mathsf{k} = \underline{t}\in\mathbb{T}_p$ and $t_{\mathsf{k}-\kappa-1} = \underline{t}-\tau_s$. For those instants, one obtains $\delta_{\mathsf{k},\kappa-1} = \tau_s$ and thus $A_{\delta_{\mathsf{k},\kappa-1}} = A_{\tau_s} = \bar{A}$ and $B_{\delta_{\mathsf{k},\kappa-1}} = B_{\tau_s} = \bar{B}$. Substituting these results into (13.43) further implies that

$$\Gamma(\underline{t}^-)\preceq\omega^{-\kappa}\left(\bar{A}\Gamma(\underline{t}-\tau_s)\bar{A}^\top + \bar{B}W\bar{B}^\top\right).$$

From the fact that $\Sigma(\underline{t}^-) = \bar{A}\Sigma(\underline{t}-\tau_s)\bar{A}^\top + \bar{B}W\bar{B}^\top$, in combination with the assumption $\Gamma(\underline{t}-\tau_s)\preceq\Sigma(\underline{t}-\tau_s)$, one can then obtain that $\Gamma(\underline{t}^-)\preceq\omega^{-\kappa}\Sigma(\underline{t}^-)$, which completes the proof of this lemma. ■

Next, let us continue with the result of Theorem 13.4, which is proven by induction. The first step is to verify that $\Gamma(\tau_s)\preceq\Sigma(\tau_s)$ when $\Gamma(0) = \Sigma(0)$. Substituting the time-periodic instant $\underline{t} = \tau_s$ into Lemma 13.1 gives that the predicted covariance matrices $\Gamma(\tau_s^-)$ and $\Sigma(\tau_s^-)$ satisfy $\Gamma(\tau_s^-)\preceq\omega^{-\kappa}\Sigma(\tau_s^-)$. The result of this latter inequality implies that after the update equations of (13.40) and (13.41) one has that $\Gamma(\tau_s)\preceq\Sigma(\tau_s)$, which completes the first step.

The second step is to show that $\Gamma(t_\mathsf{k})\preceq\Sigma(t_\mathsf{n})$ holds for any $t_\mathsf{k} = t_\mathsf{n}\in\mathbb{T}_p$, when $\Gamma(t_\mathsf{k}-\tau_s)\preceq\Sigma(t_\mathsf{n}-\tau_s)$ holds. Since $t_\mathsf{k} = t_\mathsf{n}$ is a time-periodic instant and $\Gamma(t_\mathsf{k}-\tau_s)\preceq\Sigma(t_\mathsf{n}-\tau_s)$ holds, one can employ the results of Lemma 13.1 by considering $t_\mathsf{k} = \underline{t}$ and $t_\mathsf{n} = \underline{t}$. This lemma then states that $\Gamma(t_\mathsf{k}^-)$ and $\Sigma(t_\mathsf{n}^-)$ satisfy $\Gamma(t_\mathsf{k}^-)\preceq\omega^{-\kappa}\Sigma(t_\mathsf{n}^-)$. Substituting this result in the update equations of (13.40) and (13.41) further implies that $\Gamma(t_\mathsf{k})\preceq\Sigma(t_\mathsf{n})$, which completes the second step of induction and thereby, the proof of this theorem.

Bibliography

[1] L. Aggoun and R. Elliot. *Measure Theory and Filtering*. Cambridge: Cambridge University Press, UK, 2004.

[2] A. Alessandri, M. Baglietto, and G. Battistelli. Receding-horizon estimation for discrete-time linear systems. *IEEE Transactions on Automatic Control*, 48(3):473–478, 2003.

[3] K. J. Åström and B. M. Bernhardsson. Comparison of Riemann and Lebesgue sampling for first order stochastic systems. In *Proceedings of the 41st IEEE Conf. on Decision and Control*, pages 2011–2016, Las Vegas, NV, 2002.

[4] F. L. Chernousko. *State Estimation for Dynamic Systems*. Boca Raton, FL: CRC Press, 1994.

[5] R. Cogill. Event-based control using quadratic approximate value functions. In *48th IEEE Conference on Decision and Control*, pages 5883–5888, Shanghai, China, 2009.

[6] R. E. Curry. *Estimation and Control with Quantized Measurements*. Clinton, MA: MIT Press, 1970.

[7] W. Dargie and C. Poellabauer. *Fundamentals of Wireless Sensor Networks: Theory and Practice*. Wiley, 2010.

[8] D. V. Dimarogonas and K. H. Johansson. Event-triggered control for multi-agent systems. In *Proceedings of the 48th IEEE Conference on Decision and Control*, pages 7131–7136, Shanghai, China, December 16–18, 2009.

[9] M. C. F. Donkers. *Networked and Event-Triggered Control Systems*. PhD thesis, Eindhoven University of Technology, 2012.

[10] W. P. M. H. Heemels, R. J. A. Gorter, A. van Zijl, P. P. J. van den Bosch, S. Weiland, W. H. A. Hendrix, and M. R. Vonder. Asynchronous measurement and control: A case study on motor synchronization. *Control Engineering Practice*, 7:1467–1482, 1999.

[11] T. Henningsson. Recursive state estimation for linear systems with mixed stochastic and set-bounded disturbances. In *Proceedings of the 47th IEEE Conference on Decision making and Control (CDC08)*, pages 678–683, Cancun, Mexico, December 9–11, 2008.

[12] T. Henningsson, E. Johannesson, and A. Cervin. Sporadic event-based control of first-order linear stochastic systems. *Automatica*, 44(11):2890–2895, 2008.

[13] O. C. Imer and T. Basar. Optimal estimation with limited measurements. In *Proceedings of the 44th IEEE Conference on Decision and Control*, pages 1029–1034, Seville, Spain, December 13–15, 2005.

[14] O. C. Imer and T. Basar. Optimal control with limited controls. In *American Control Conference*, pages 298–303, Minneapolis, MN, June 14–16, 2006.

[15] H. L. Lebesgue. Integrale, longueur, aire. PhD thesis, University of Nancy, 1902.

[16] D. Lehmann and J. Lunze. A state-feedback approach to event-based control. *Automatica*, 46:211–215, 2010.

[17] G. V. Moustakides, M. Rabi, and J. S. Baras. Multiple sampling for estimation on a finite horizon. In *Proceedings of the 45th IEEE Conference on Decision and Control*, pages 1351–1357, San Diego, CA, December 13–15, 2006.

[18] R. Mahler. General Bayes filtering of quantized measurements. In *Proceedings of the 14th International Conference on Information Fusion*, pages 346–352, Chicago, IL, July 5–8, 2011.

[19] M. Mallick, S. Coraluppi, and C. Carthel. Advances in asynchronous and decentralized estimation. In *Proceeding of the 2001 Aerospace Conference*, Big Sky, MT, March 10–17, 2001.

[20] J. W. Marck and J. Sijs. Relevant sampling applied to event-based state-estimation. In *Proceedings of the 4th International Conference on Sensor Technologies and Applications*, pages 618–624, Venice, Italy, July 18–25, 2010.

[21] K. V. Mardia, J. T. Kent, and J. M. Bibby. *Multivariate Analysis*. Academic Press, London, 1979.

[22] M. Miskowicz. Send-on-delta concept: An event-based data-reporting strategy. *Sensors*, 6:49–63, 2006.

[23] M. Miskowicz. Asymptotic effectiveness of the event-based sampling according to the integral criterion. *Sensors*, 7:16–37, 2007.

[24] P. Morerio, M. Pompei, L. Marcenaro, and C. S. Regazzoni. Exploiting an event based state estimator in presence of sparse measurements in video analytics. In *Proceedings of the 2014 International Conference on Acoustics, Speech and Signal Processing (ICASSP)*, pages 1871–1875, Florence, Italy, May 4–9, 2014.

[25] V. H. Nguyen and Y. S. Suh. Improving estimation performance in networked control systems applying the send-on-delta transmission method. *Sensors*, 7:2128–2138, 2007.

[26] B. Noack, F. Pfaff, and U. D. Hanebeck. Optimal Kalman gains for combined stochastic and set-membership state estimation. In *Proceedings of the 51st IEEE Conference on Decision and Control (CDC 2012)*, pages 4035–4040, Maui, HI, December 10–13, 2012.

[27] B. Saltik. Output feedback control of linear systems with event-triggered measurements. Master thesis, University of Technology, Eindhoven, 2013.

[28] D. Shi, T. Chen, and L. Shi. An event-triggered approach to state estimation with multiple point- and set-valued measurements. *Automatica*, 50(6):1641–1648, 2014.

[29] J. Sijs. State estimation in networked systems. PhD thesis, Eindhoven University of Technology, 2012.

[30] J. Sijs and M. Lazar. Event based state estimation with time synchronous updates. *IEEE Transactions on Automatic Control*, 57(10):2650–2655, 2012.

[31] B. Sinopoli, L. Schenato, M. Franceschetti, K. Poolla, M. Jordan, and S. Sastry. Kalman filter with intermittent observations. *IEEE Transactions on Automatic Control*, 49:1453–1464, 2004.

[32] H. W. Sorenson and D. L. Alspach. Recursive Bayesian estimation using Gaussian sums. *Automatica*, 7:465–479, 1971.

[33] C. Stocker. *Event-Based State-Feedback Control of Physically Interconnected Systems*. Berlin: Logos Verlag Berlin Gmbh, 2014.

[34] S. Trimpe and R. D'Andrea. An experimental demonstration of a distributed and event-based state estimation algorithm. In *Proceedings of the 18th IFAC World Congress*, pages 8811–8818, Milan, Italy, August 28–September 2, 2011.

[35] S. Trimpe and R. D'Andrea. Event-based state estimation with variance-based triggering. In *Proceedings of the 51st IEEE Conference on Decision and Control (CDC 2012)*, pages 6583–6590, Maui, HI, December 10–13, 2012.

[36] J. Wu, K. H. Johansson, and L. Shi. Event-based sensor data scheduling: Trade-off between communication rate and estimation quality. *IEEE Transactions on Automatic Control*, 58(4):1041–1046, 2013.

[37] Y. Xu and J. P. Hespanha. Optimal communication logics for networked control systems. In *Proceedings of the 43rd IEEE Conference on Decision and Control*, pages 3527–3532, Paradise Island, Bahamas, December 14–17, 2004.